Article

4-(3-Aminoazetidin-1-yl)pyrimidin-2-amines as high-affinity non-imidazole histamine H3 receptor agonists with in vivo central nervous system activity

Gábor Wágner, Tamara Mocking, Marta Arimont, Gustavo Provensi, Barbara Rani, Bruna Silva-Marques, Gniewomir Latacz, Daniel Da Costa Pereira, Christina Karatzidou, Henry F. Vischer, Maikel Wijtmans, Katarzyna Kiec-Kononowicz, Iwan J. P. De Esch, and Rob Leurs

Just Accepted

4-(3-Aminoazetidin-1-yl)pyrimidin-2-amines as high-affinity non-imidazole histamine H$_3$ receptor agonists with *in vivo* central nervous system activity

Gábor Wágner,[a] Tamara A. M. Mocking,[a] Marta Arimont,[a] Gustavo Provensi,[b] Barbara Rani,[c] Bruna Silva-Marques,[b,d] Gniewomir Latacz,[e] Daniel Da Costa Pereira,[a] Christina Karatzidou,[a] Henry F. Vischer,[a] Maikel Wijtmans,[a] Katarzyna Kieć-Kononowicz,[e] Iwan J. P. de Esch[a] and Rob Leurs[a]*

[a]Amsterdam Institute for Molecules, Medicines and Systems (AIMMS), Division of Medicinal Chemistry, Faculty of Science, Vrije Universiteit Amsterdam, De Boelelaan 1108, 1081 HZ Amsterdam, The Netherlands.

[b] Department of Neuroscience, Psychology, Drug Research and Child Health, Section of Pharmacology and Toxicology, University of Florence, Viale G. Pieraccini 6, CAP 50139, Florence, Italy.

c Department of Health Sciences, University of Florence, Viale G. Pieraccini 6, CAP

50139, Florence, Italy.

d Department of Physiotherapy, Federal University of São Carlos, Washington Luís, km

235, SP-310, São Carlos, Brazil.

e Department of Technology and Biotechnology of Drugs, Medical College, Jagiellonian

University, Medyczna 9, PL 30-688 Cracow, Poland

ABSTRACT: Despite the high diversity of histamine H_3 receptor (H_3R) antagonist/inverse

agonist structures, partial or full H_3R agonists have typically been imidazole derivatives.

An in-house screening campaign intriguingly afforded the non-imidazole 4-(3-azetidin-1-

yl)pyrimidin-2-amine **11b** as partial H_3R agonist. Here, the design, synthesis and

structure-activity relationships of **11b** analogues are described. This series yields several

non-imidazole full agonists with potencies varying with the alkyl substitution pattern on

the basic amine following the *in vitro* evaluation of H_3R agonism using a CRE-luciferase

reporter gene assay. Key compound VUF16839 (**14d**), combines nanomolar on-target

activity (pK_i = 8.5, pEC_{50} = 9.5) with weak activity on CYP enzymes and good metabolic

stability. The proposed H_3R binding mode of **14d** indicates key interactions similar to

those attained by histamine. *In vivo* evaluation of **14d** in a social recognition test in mice,

revealed an amnesic effect at 5 mg/kg i.p. The excellent *in vitro* and *in vivo*

pharmacological profile and the non-imidazole structure of **14d** make it a promising tool

compound in H_3R research.

INTRODUCTION

The four histamine receptors (H_1R, H_2R, H_3R, H_4R) belong to class A of the G protein-coupled receptor (GPCR) family.[1] The histamine H_3 receptor (H_3R) was discovered in 1983 by Arrang *et al.*[2] and regulates the release of several neurotransmitters such as histamine (**1**), acetylcholine, serotonin, noradrenaline and dopamine, both as auto- and heteroreceptor.[1] Due to its expression in cortex, striatum and hippocampus, H_3R regulates several physiological processes such as sleep-wake regulation, cognition and food intake.[1,3]

During the early years of discovery of H_3R ligands, the natural ligand histamine served as an initial structure for drug design, leading to a plethora of imidazole-containing ligands. However, imidazole-containing ligands are associated with drug-drug interactions due to the propensity for cytochrome P450 (CYP) inhibition and with poor brain penetration.[4,5] Therefore, research towards therapeutically relevant H_3R antagonists focused on drug-like non-imidazole structures[6,7] and these efforts have led to numerous clinical candidates for different indications connected to central nervous

system diseases, e.g., Alzheimer`s disease, Attention Deficit Hyperactivity Disorders,

sleep disorders, schizophrenia, obesity, epilepsy and neuropathic pain and narcolepsy.[8,9]

For the latter condition, the H_3R ligand pitolisant (Wakix®) was approved by the EMA in

2016,[10] and most recently, by the FDA in 2019.[11]

In sharp contrast, developing non-imidazole H_3R agonists has not been very successful.

The best agonists contain an imidazole ring[12,13,22,23,14–21] and, compared to the

endogenous ligand histamine (**1**), these derivatives show similar (e.g. imbutamine (**2**)) or

significantly higher affinity (pK_i) and/or functional activity (pEC_{50}) on H_3R (e.g. imetit (**3**),

methimepip (**4**) and AEIC (**5**)) (Fig. 1A). Imidazole-containing agonists have shown some

potential application in different therapeutic areas, such as mechanical nociception,[23]

obesity and diabetes mellitus (diet-induced obesity mice test)[24] and stress (rodent-

intruder mice test).[21] Some data also support the hypothesis of cardioprotective effect of

H_3R receptor activation.[25,26] However, it is fair to say that imidazole-containing agonists

may suffer from the same imidazole-related drawbacks that were associated with the first

generation of imidazole-containing H_3R antagonists (*vide supra*). Future studies on the

pharmacological and therapeutic role of H_3R agonists can therefore be helped by having non-imidazole H_3R agonists available.

A very limited number of non-imidazole agonists has been published to date (Fig. 1B). VUF8430 (**6**) was designed as an H_4R agonist based on the H_2R agonist dimaprit, and shows micromolar affinity and full H_3R agonism as well.[27] The histamine analogues amthamine (**7a**) and amselamine (**7b**) were identified as H_2R agonists, but both show weak H_3R agonist activity in an electrically stimulated guinea-pig jejunum model.[28,29] Three pentacyclic spiroindolinone derivatives were isolated from *Penicillium waksmanii*, of which PF1270A (**8**) shows the best affinity for H_3R and moderate functional H_3R activity in a GTPγS accumulation assay.[30] ZEL-H16 (**9**) has been reported to have nanomolar binding affinity to the H_3R, partial H_3R agonism in forskolin-stimulated cAMP accumulation and ERK1/2 signaling assays, and full H_3R agonism in guinea-pig ileum contraction assay.[31] Finally, a compound set with 94 examples in 4 compound families with either a β-lactam or pyrrolidinone central core without basic amino moiety was published recently and surprisingly included compounds with nanomolar functional H_3R agonist activities (e.g. compound **10**).[32] The fungal isolates and the multi-component reaction product **10**

are large and complex molecules, which are difficult to align with known H_3R

pharmacophores or H_3R binding modes for agonists and antagonists. We therefore

started a search for novel high-affinity non-imidazole H_3R full agonists with simpler

structures to generate fundamental knowledge on ligand recognition and signaling of the

H_3R.

A

Histamine (**1**)
pK$_i$: 8.0
pEC$_{50}$: 8.3 (β-gal)
α: 1.0 (β-gal)

Imbutamine (**2**)
pK$_i$: 8.4
pEC$_{50}$: 8.3 (cAMP)
α: 1.0 (cAMP)

Imetit (**3**)
pK$_i$: 8.8
pEC$_{50}$: 9.9 (β-gal)
α: 1.0 (β-gal)

Methimepip (**4**)
pK$_i$: 9.0
pEC$_{50}$: 9.5 (β-gal)
α: 0.8 (β-gal)

AEIC (**5**)
pK$_i$: 8.8
pEC$_{50}$: 8.0 (cAMP)

B

VUF8430 (**6**)
pK$_i$: 6.0
pEC$_{50}$: 6.5 (β-gal)
α: 1.0 (β-gal)

A = S: Amthamine (**7a**)
pD$_2$: 4.7 (gp jejunum)
A = Se: Amselamine (**7b**)
pD$_2$: 4.4 (gp jejunum)

PF1270A (**8**)
pK$_i$: 7.3
pEC$_{50}$: 6.9 (GTPγS)

ZEL-H16 (**9**)
pK$_i$: 8.7
pEC$_{50}$: 8.4 (cAMP)
α: 0.6 (cAMP)

CSIR compound (**10**)
pEC$_{50}$: 8.6 (cAMP)

Figure 1. A) Representative imidazole H_3R agonists. Activities are extracted from Igel *et al.*[33], Govoni *et al.*[18] and Kazuta *et al.*[12] **B**) Published non-imidazole H_3R (partial)

agonists.[27–32] Unless mentioned otherwise, compounds were tested on the human

receptor. α: intrinsic activity compared to histamine. β-gal: CRE-β-galactosidase reporter

gene assay; *c*AMP: forskolin-stimulated *c*AMP accumulation assay.

RESULTS

Design

During an in-house compound screen aimed at identifying agonist activities in a set of

ligands using a H_3R-driven reporter gene assay in HEK293T cells, diaminopyrimidine **11b**

emerged as a H_3R partial agonist hit (α = 0.7), while its close derivative **11i** showed only

weak agonist activity (α = 0.4) (Fig. 2A). Interestingly, a set of four diaminopyrimidine

compounds has been tested before by others on H_3R *en route* to imbutamine (**2**)

analogues, but the majority of these diaminopyrimidines were rather inactive and, where

applicable, all were shown to be antagonists/inverse agonists.[34] Intrigued by the agonist

activity of the diaminopyrimidine **11b** and recognizing its core as a thoroughly explored

heterocycle in the H_4R area,[35] we decided to perform an in-depth patent search on this

scaffold in an effort to capture the full array of industrial contributions. This resulted in the

identification of **14a** (Fig. 2B) as closest derivative with data associated to H_3R (Fig. 2B).[36]

Remarkably, **14a** was claimed as an H_3R agonist by Abbott, although its actual synthesis

was not included and only the potential synthetic route was described.[36] In the same

patent 25 related examples have been prepared and partial agonism at the human H_3R

is reported.[36]

Based on **11b** and **14a**, we designed a focused series of compounds to explore the H_3R

affinity and activity in the chemical space between **14a** and **11b** (Fig. 2B). The design

strategy targets four series with *i*Pr, Et, Me or H as R^1 group at position 6 (**11-14**). These

R^1 groups were combined with different substituents on the basic amino groups (R^2 and

R^3). Beyond the evident H (**a**) and Me (**b**) substituents, dimethyl derivatives (**i**) were

synthesized due to the potential functional switch that appears to reside in the case of

11b and **11i**. Based on the initial results of the designed compound set (*vide infra*), the

R^1=H series was extended with elongated (**d**, **f**), branched (**e**, **g**, **h**) and disubstituted (**j**, **k**)

amino derivatives. This second design iteration was also inspired by previous work from

our labs on the imidazole-containing agonist imbutamine (**2**), which harbors a functional

switch on the basic amine.[18] Beyond **14a**, some exact compounds from this designed set

are known but none in a context of H_3R. That is **11a**, **11b**, **12b**, have been claimed as H_4R

ligands,[37,38] while **12i**, **13i**, **14i**, **14j** and **14k** were offered in chemical catalogues (April

2019) without any synthesis description, analytical or pharmacological data.

1
2
3
4
5
6
7
8
9
10
11
12
13
14
15
16
17
18
19
20
21
22
23
24
25
26
27
28
29
30
31
32
33
34
35
36
37
38
39
40
41
42
43
44
45
46
47
48
49
50
51
52
53
54
55
56
57
58
59
60
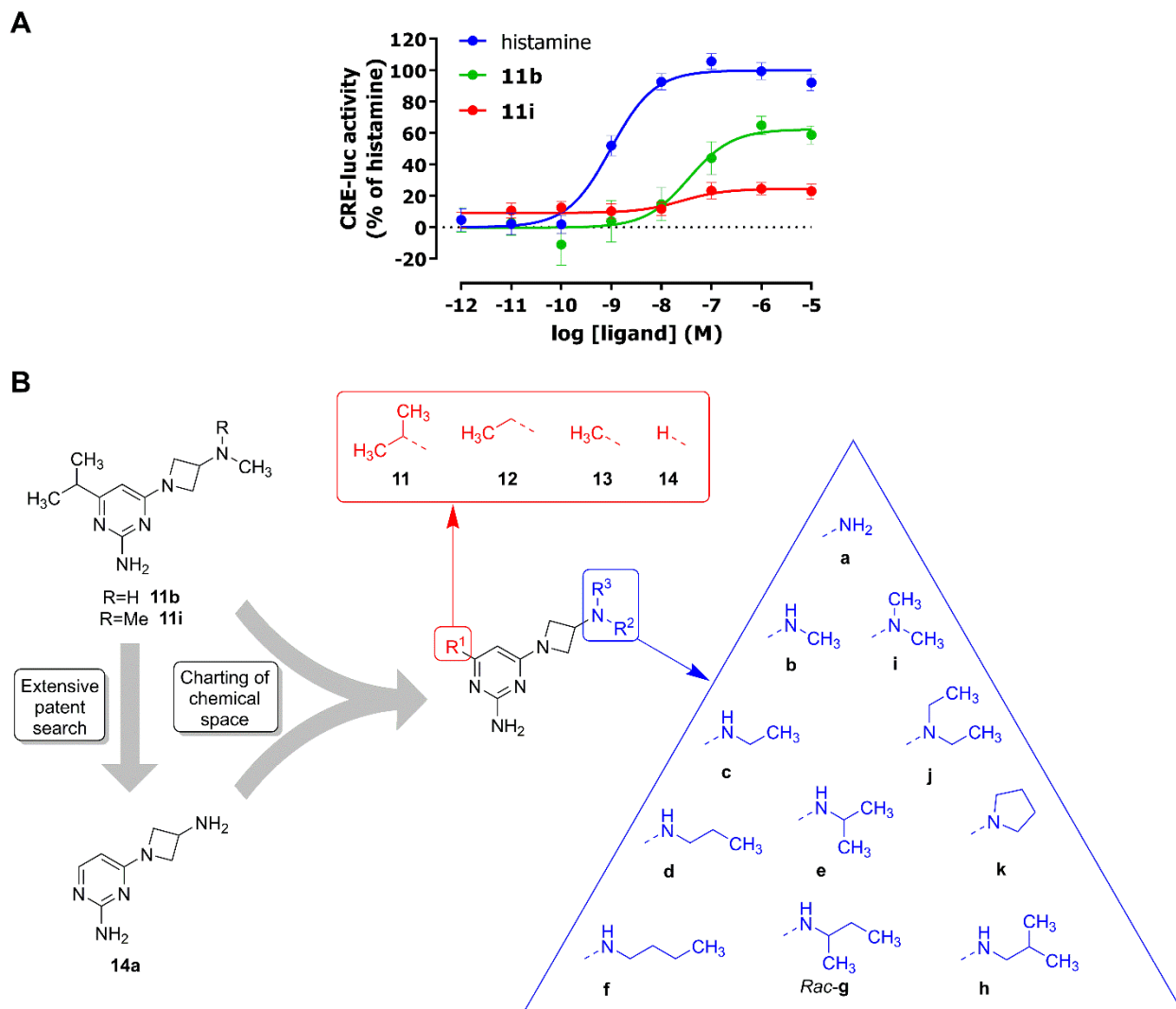
Figure 2. A) Initial functional data of compound **11b** and **11i** compared to histamine, as obtained by ligand-induced activation of hH$_3$R expressed on HEK293T cells measured by CRE-luc reporter gene assay. Shown is a representative graph of at least 3 experiments performed in triplicate. Data are mean ± S.D. **B)** Structures of **11b** and **11i**, the closest relevant structure (**14a**) resulting from a subsequent extensive patent search and the compound set designed for the current study.

1
2
3
4
5
6
7
8
9
10
11
12
13
14
15
16
17
18
19
20
21
22
23
24
25
26
27
28
29
30
31
32
33
34
35
36
37
38
39
40
41
42
43
44
45
46
47
48
49
50
51
52
53
54
55
56
57
58
59
60

Chemistry

The designed compound set shown in Fig. 2B was synthesized as outlined in Scheme 1. The key step of the synthetic route was a nucleophilic aromatic substitution on the appropriate aromatic cores with aminoazetidine moieties (step ii). The 4-chloro-2-aminopyrimidines were commercially available (**19**, **20**) or were synthesized (**17**, **18**) from the appropriate pyrimidin-4(3H)-one derivatives (**15**, **16**) with $POCl_3$. The R^2=H or Me derivatives of the Boc-protected 3-aminoazetidines (**28a, b**) were commercially available, while the R^2=Et, *n*Pr, *n*Bu derivatives were synthesized. These intermediates were built up from benzhydryl-protected 3-aminoazetidine (**25**) with Boc protection of the primary amino group to give **26**, followed by alkylation with the corresponding iodoalkyl reagents resulting in the orthogonally protected intermediates (**27c, d**, **f**) and the removal of the benzhydryl group with hydrogenation. The resulting mixtures of unprotected azetidine intermediate and diphenylmethane were used directly for the ensuing nucleophilic substitution with **17-20**. The key nucleophilic aromatic substitution of the appropriate Boc-protected intermediates was performed in a microwave at 120 - 150 °C to give **21-24**. This was followed by the deprotection under acidic condition to afford the majority of

monosubstituted (R^2=H or linear alkyl, R^3=H) products **11-14**. Although the Boc-protection

was necessary at the precursor stage to avoid overalkylation in case of linear alkyl

derivatives, overalkylation was not a problem in case of the branched-alkyl derivatives as

a result of steric hindrance. Therefore, the branched-alkyl derivatives **14e**, **g**, **h** as well as

the dialkylated derivatives **12i**, **13i**, **14i** and **14j** were synthesized from **14a** with a reductive

amination. Last, **11i** was synthesized directly from **17** and N,N-dimethylazetidin-3-amine

with a nucleophilic substitution, while the pyrrolidine ring of **14k** was obtained from 1,4-

diiodobutane and **14a**.

Scheme 1. Reagents and conditions: i) POCl$_3$, 110 °C, 3h, 26-52 %; ii) DIPEA, dioxane or NMP, μW, 120 - 150 °C, 0.5 - 2 h, 27-50 % (**a** and **b**) or 35-71 % (**c**, **d** and **f**, two steps from benzhydryl deprotection); iii) HCl, DCM, MeOH, rt - 50 °C, 3 h - overnight, 10 % - quant.; iv) aldehyde/ketone, AcOH, NaHB(OAc)$_3$, DCM, MeOH, rt, 3 h - overnight, 16-44 %; or 1,4-diiodobutane, K$_2$CO$_3$, MeCN, reflux, 16 h, 9 %; v) *N,N*-dimethylazetidin-3-amine dihydrochloride, DIPEA, dioxane, μW, 150 °C, 30 min, 65 %; vi) di-*tert*-butyl dicarbonate, TEA, THF, rt, overnight, 63 %; vii) NaH, R^{2}I, THF, 0 °C - rt, overnight, 28-58 %; viii) H$_2$, Pd/C, MeOH, EtOH, rt - 60 °C, 1 h - overnight, not purified and used crude.

Pharmacological evaluation

The synthesized compound set was tested for their activity at the human H$_3$R transiently expressed in HEK293T cells. Binding affinity (K$_i$) was evaluated using a [^{3}H]NAMH displacement assay, while potency (EC$_{50}$) and intrinsic activity (α) were determined as the H$_3$R-mediated inhibition of forskolin-induced CRE-driven luciferase reporter gene activity with histamine as control (Table 1, Fig. 3). During the first iteration, the isopropyl
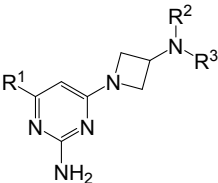
group of **11b** was gradually decreased in size to give **11**-**14**, which were all combined with small-size R^2/R^3 amino substituents (**a**, **b**, **c**, **i**). The affinities of the unsubstituted derivatives (**14**) stand out especially within the monomethylated (**b**) and monoethylated series (**c**), with both **14b** and **14c** exceeding the affinity of histamine. Although monomethylated (**b**) derivatives generally show the highest affinities in each R^1 subseries **11**-**14**, the most notable variation was observed in case of the monoethylated series **c**, with affinities of Me/Et/*i*Pr derivatives **11c**, **12c** and **13c** being considerably reduced compared to **14c** (Fig. 3A). A more indicative trend was observed in case of the functional results of this **c** series. Compound **14c** has a higher potency than **14b** and produces the same intrinsic activity (α) as histamine but with higher potency (EC_{50}), while **12c** and **13c** show more than >1 log unit weaker EC_{50} albeit with maintained full agonism ($\alpha{\sim}1.0$). Interestingly, isopropyl substitution on the R^1 position (**11c**) turns this full agonism to partial agonism ($\alpha{=}0.3$) (Fig. 3B). A similar trend was observed in the other three series, with the pyrimidine derivatives bearing $R^1{=}H$ (**14a-c**, **i**) reaching or exceeding the affinity (K_i) and potency (EC_{50}) of histamine, while any alkyl substituent at position 6 (R^1) on the pyrimidine leads to inferior results. The intrinsic activity (α) indicates full or almost full

agonism ($\alpha \geq 0.8$) in the methyl (**12a**, **b**, **i**) and ethyl (**13a**, **b**, **i**) series, while it drops to

partial agonism in the isopropyl series (**11a**, **b**, **i**) (Table 1).

Due to the better results of the pyrimidines lacking a R^1-substituent (**14**), in a

subsequent iteration the amine NHR^2 substituent was replaced with longer linear groups

(**14d**, **f**), branched groups (**14e**, **g**, **h**), or dialkylamino (**14j**, **k**) moieties. Representative

curves illustrate the SAR (Fig. 3C) and SFR (Fig. 3D) of this series. The *n*Pr derivative

14d shows the highest affinity ($pK_i=8.5$) from all linear monoalkyl substituents. Although

both shorter and longer R^2 moieties resulted in lower binding affinities (e.g. **14c**: $pK_i=8.0$

or **14f**: $pK_i=7.8$), all derivatives remained in the same affinity range (Fig. 3C). The

branched alkyl moieties as well as the dialkylated derivatives display loss of affinity

(compare e.g. **14d** vs **14e**, or **14b** vs **14i**). The potencies (EC_{50}) show almost the same

trends as observed for the affinities (Fig. 3D). Highly noteworthy, the potency of **14d**

($pEC_{50}=9.5$) is almost a log unit higher than that of histamine ($pEC_{50}=8.6$), while chain

shortening (e.g. **14b, c**), chain lengthening (**14f**), chain branching (e.g. **14e**), or

dialkylation (e.g. **14i**) results in lower potencies. In contrast to the observed differences in

affinity and potency, the intrinsic activities indicate that all derivatives of **14** remain full

agonists ($\alpha \geq 1.0$) (Table 1). A combination of highest affinity ($pK_i=8.5$), highest potency

($pEC_{50}=9.5$) and full agonism resides in **14d**. The potential aggregation of GPCR ligands

might cause nonspecific effect on the receptor activity,[39] but nephelometry revealed no

microprecipitation of **14d** up to 100 mM concentration (Fig. S1) and underscores the high

aqueous solubility of **14d** (soluble up to at least 100 mM in 50 mM Tris-HCl, pH 7.4). All

this led to identification of **14d** as key compound (VUF16839) in this study.

Table 1. Pharmacological evaluation of designed compound set. Affinity values (pK_i) were determined by [³H]NAMH displacement assay on hH_3R expressed on HEK293T cell homogenates. Potency (pEC_{50}) and intrinsic activity (α) were determined by ligand induced activation of hH_3R expressed on HEK293T cells as measured by a CRE-luciferase reporter gene assay. Data are mean ± S.E.M. of at least 3 experiments performed in triplicate.

Compound	R¹	R²	R³	pK_i	pEC_{50}	α
Histamine	-	-	-	7.9 ± 0.2	8.6 ± 0.0	1.0 ± 0.0
11a	*i*Pr	H	H	6.7 ± 0.0	7.1 ± 0.1	0.7 ± 0.0
11b	*i*Pr	Me	H	7.0 ± 0.0	7.9 ± 0.4	0.7 ± 0.1
11c	*i*Pr	Et	H	7.0 ± 0.1	6.8 ± 0.3	0.3 ± 0.1

11i	*i*Pr	Me	Me	6.9 ± 0.0	7.0 ± 0.2	0.4 ± 0.0
12a	Et	H	H	7.1 ± 0.0	7.5 ± 0.0	0.9 ± 0.0
12b	Et	Me	H	7.3 ± 0.1	7.6 ± 0.0	0.8 ± 0.0
12c	Et	Et	H	6.9 ± 0.1	7.5 ± 0.1	0.9 ± 0.0
12i	Et	Me	Me	6.6 ± 0.2	7.2 ± 0.1	0.8 ± 0.0
13a	Me	H	H	7.3 ± 0.1	7.8 ± 0.0	0.9 ± 0.0
13b[b]	Me	Me	H	7.5 ± 0.1	8.0 ± 0.0	0.8 ± 0.1
13c	Me	Et	H	7.1 ± 0.1	7.9 ± 0.0	1.0 ± 0.0
13i	Me	Me	Me	6.5 ± 0.2	7.4 ± 0.0	0.9 ± 0.1
14a[a]	H	H	H	7.8 ± 0.1	8.3 ± 0.0	1.1 ± 0.0
14b[a]	H	Me	H	8.2 ± 0.1	8.9 ± 0.1	1.1 ± 0.1

14c[a]	H	Et	H	8.0 ± 0.1	9.2 ± 0.0	1.0 ± 0.1
14d[a]	H	*n*Pr	H	8.5 ± 0.1	9.5 ± 0.1	1.2 ± 0.1
14e[a]	H	*i*Pr	H	7.4 ± 0.1	8.5 ± 0.1	1.2 ± 0.1
14f[a]	H	*n*Bu	H	7.8 ± 0.1	9.1 ± 0.3	1.2 ± 0.0
14g[a]	H	*rac-s*Bu	H	7.9 ± 0.2	8.7 ± 0.1	1.1 ± 0.0
14h[a]	H	*i*Bu	H	7.4 ± 0.2	8.3 ± 0.0	1.1 ± 0.0
14i[a]	H	Me	Me	7.3 ± 0.1	8.4 ± 0.1	1.0 ± 0.1
14j[a]	H	Et	Et	7.2 ± 0.1	8.1 ± 0.1	1.2 ± 0.1
14k[a]	H	NR^2R^3 = Pyrrolidine		7.4 ± 0.1	8.1 ± 0.0	1.3 ± 0.2

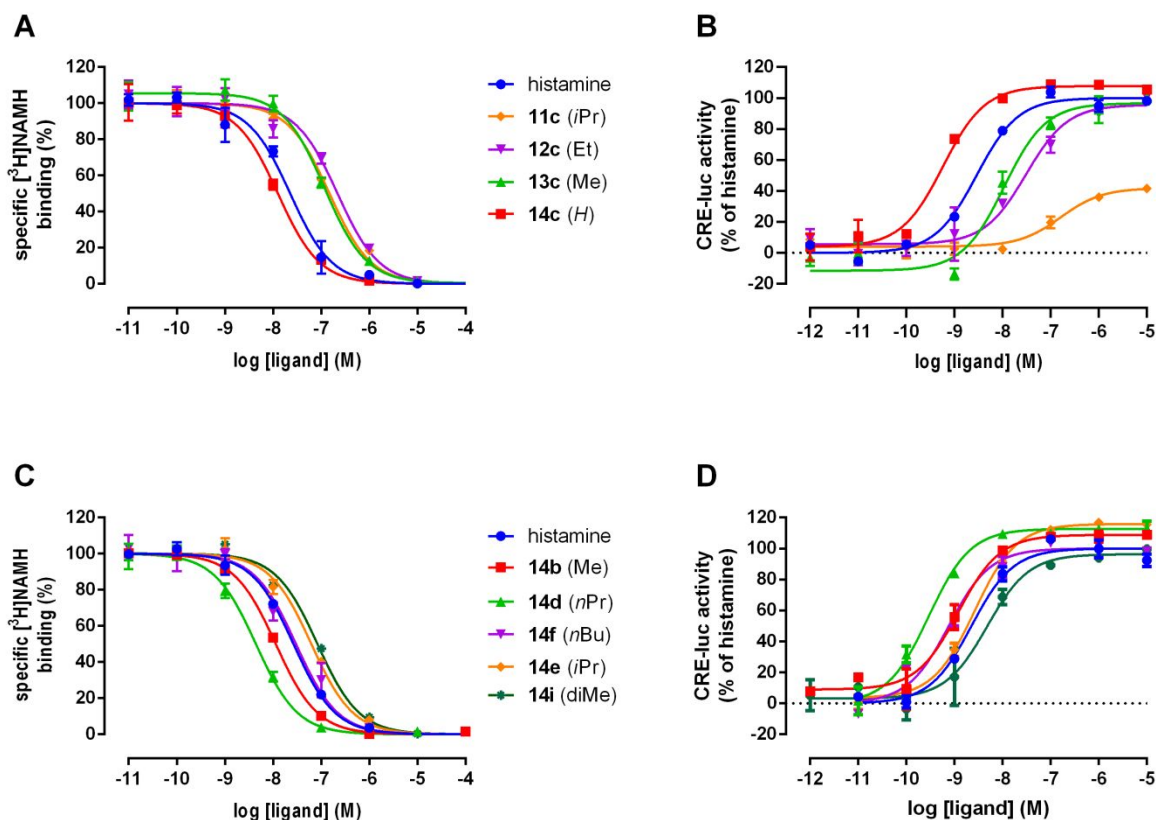[a] Measured as fumarate salt.

[b] Measured as dihydrochloride salt.

Figure 3. Representative Structure-Affinity (**A**, **C**) and Structure-Function relationship (**B**,

D) effects selected from Table 1. (**A**, **B**) Different R^1 substituents with R^2 = Et and R^3 = H

(**11c**, **12c**, **13c**, **14c**); (**C**, **D**) Different R^2 and R^3 substituents with R^1 = H (**14b**, **14d**, **14e**,

14f, **14i**). Shown is a representative graph of at least 3 experiments performed in triplicate.

Data are mean ± S.D.

Computational studies of 14d.

A combination of molecular docking and molecular dynamics simulations was used in order to evaluate the potential binding mode of the key compound **14d** and to compare it to the binding mode of the endogenous ligand histamine. A homology model of H_3R based on the available crystal structure of H_1R was used (see Experimental section). This model was validated by its ability to retrospectively discriminate between known H_3R fragment-like ligands and true inactives.[40] Histamine was docked in the receptor model using PLANTS 1.1 (Fig. 4A). The best-scored docking pose showing interactions with both D114$^{3.32}$ and E206$^{5.461}$ (residues known to be involved in H_3R ligand binding[40–45]) was selected. During 100 ns of molecular dynamics (MD) simulations, histamine is able to maintain stable interactions with residues D114$^{3.32}$ and E206$^{5.461}$ as well as with Y374$^{6.51}$ (Fig. 4B and 4E). Using similar procedures, compound **14d** was also docked into the same homology model using PLANTS 1.1 (Fig. 4A) and the best scored docking results show similar interactions of **14d** with D114$^{3.32}$ and E206$^{5.461}$. The basic amine of **14d** forms an ionic interaction with the negatively-charged side chain of D114$^{3.32}$, and the amino group in the pyrimidine ring makes a hydrogen bond with E206$^{5.461}$. Different docking poses maintain these key interactions but show a different positioning of the linear *n*Pr

moiety at the R^2 position: towards the extracellular surface of the receptor or towards the intracellular side (Fig. S2A and Fig. S2B, respectively). MD simulations of the two alternative models were performed (Supplementary Movies 1 and 2). The model in which the *n*Pr group of **14d** is directed towards the intracellular half of the receptor was not stable along 100 ns of MD simulations (Fig. S2D, Supplementary Movie 2), while the model where the *n*Pr group of **14d** is pointing towards the extracellular vestibule remained stable throughout the entire simulation time (Fig. S2C, Supplementary Movie 1). This binding mode is shown in Fig. 4D and the interactions that remained stable during the simulations are depicted in Fig. 4C and the interaction finger prints (IFP) in Fig. 4E. It can be concluded that the non-imidazole H_3R ligand **14d** exerts its unusual agonist H_3R activity by showing a similar pharmacophore as the endogenous H_3R ligand. That is, it may achieve its agonist activity by forming similar interactions with the same residues as histamine.
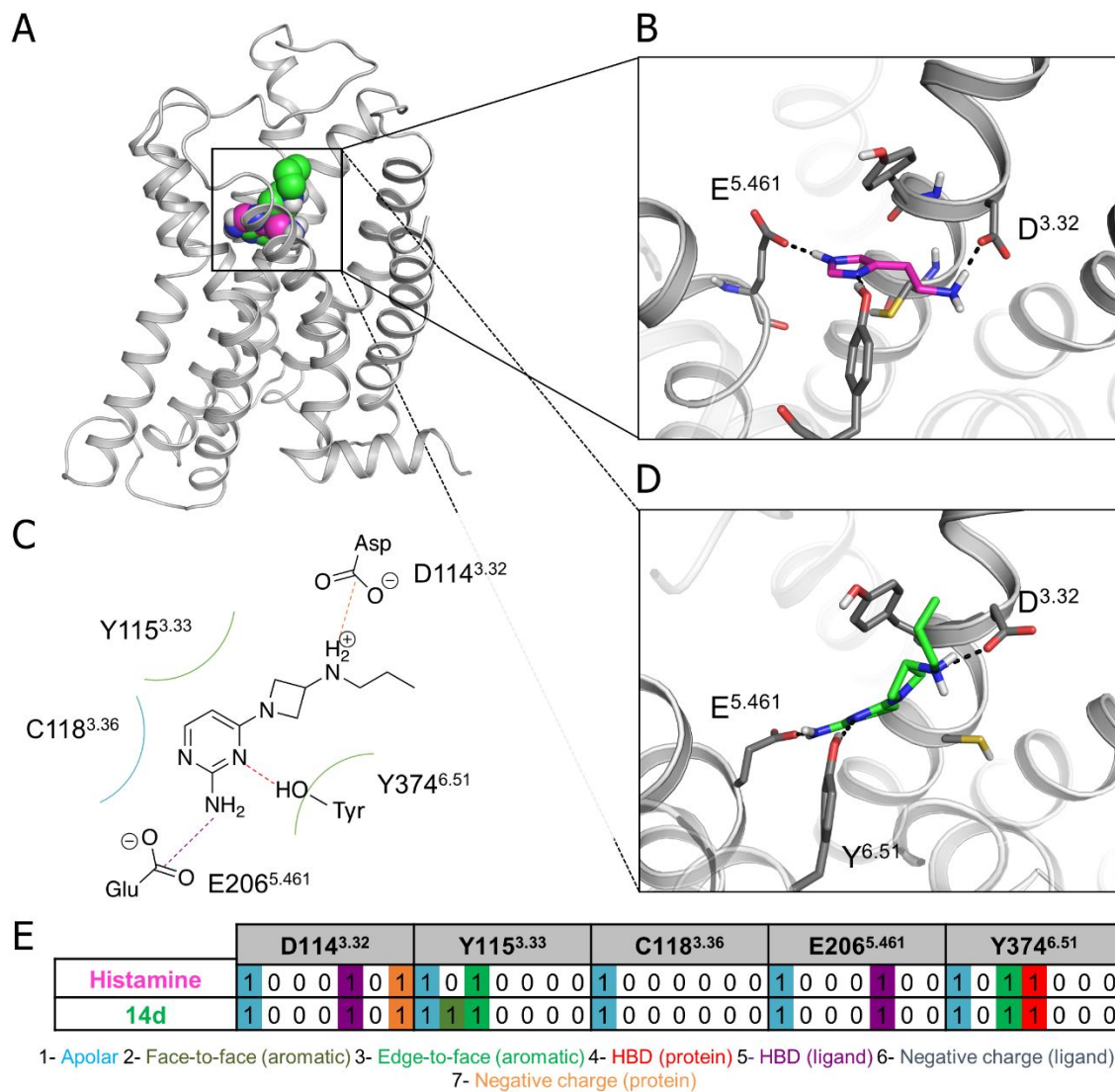
Figure 4. Predicted binding mode of **14d**. **A**) Overview of the H$_3$R homology model based on the H$_1$R crystal structure (PDB ID: 3RZE).[46] The experimentally validated binding mode of histamine (magenta) is shown in more detail in (**B**) and the predicted binding mode of **14d** (green) is schematically represented in (**C**) and shown in more detail in (**D**).

1
2
3
4
5
6
7
8
9
10
11
12
13
14
15
16
17
18
19
20
21
22
23
24
25
26
27
28
29
30
31
32
33
34
35
36
37
38
39
40
41
42
43
44
45
46
47
48
49
50
51
52
53
54
55
56
57
58
59
60

Interaction fingerprint representations of histamine and compound **14d** are shown in (**E**),

where a one represents the presence of an interaction according to the color coding: blue

for apolar, dark green for face-to-face aromatic, green for edge-to-face aromatic, red for

protein hydrogen bond donor, purple for ligand hydrogen bond donor, grey for ligand

negative charge, and orange for protein negative charge.

Pharmacological and pharmacokinetic characterization of 14d.

Functional characterization of key compound **14d** in a direct G protein activation assay,

i.e. [^{35}S]-GTPγS accumulation assay on hH$_3$R expressing cell homogenates (Fig. 5A),

results in potent, but partial agonism (pEC$_{50}$ = 8.4 ± 0.3, α = 0.5 ± 0.05) compared to
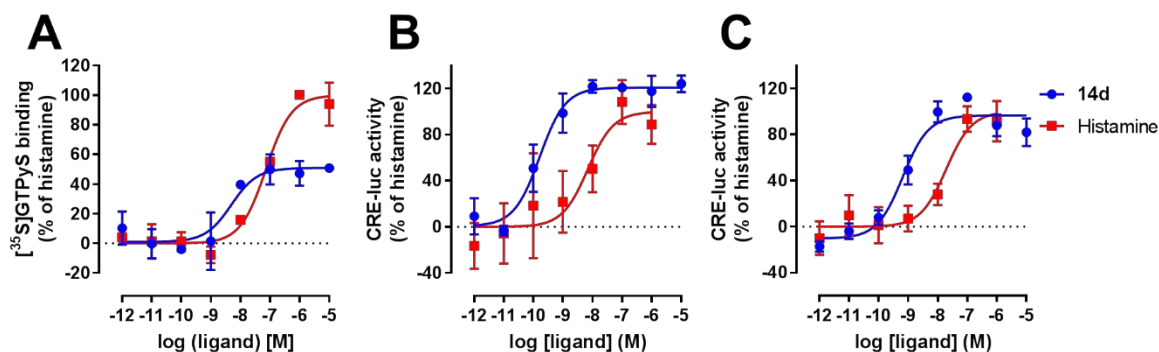
histamine (pEC$_{50}$ = 7.2 ± 0.3, α = 1.0 ± 0.0).

Figure 5. (**A**) Dose-dependent $G\alpha_i$ activation by **14d** and histamine as measured by $[^{35}S]GTP\gamma S$ accumulation on HEK293T cell homogenates expressing the hH_3R. (**B, C**) Dose-response curves of **14d** and histamine for ligand-induced activation of mH_3R (**B**) and mH_4R (**C**) expressed on HEK293T cells as measured by CRE-luciferase reporter gene assay. Representative graphs of at least three experiments performed in triplicate are shown. Data are mean ± S.D.

Due to the high homology of the hH_3R with hH_4R (43 % full sequence identity, 58 % predicted transmembrane regions identity),[47] several, mainly imidazole-containing, hH_3R ligands are known to possess high affinity for hH_4R as well,[33,44] although there are examples of imidazole-containing H_3R agonists with high H_3R/H_4R selectivity as well (e.g., **4** and **5**).[12,33] Therefore, **14d** was tested for its H_3R/H_4R selectivity. The pyrimidine shows only marginal selectivity with respect to binding hH_3R or hH_4R (hH_3R pK_i = 8.5 ± 0.1 vs hH_4R pK_i = 8.1 ± 0.0), but encouragingly a 10-fold selectivity in potency is observed in favour of the hH_3R (hH_3R pEC_{50} = 9.5 ± 0.1 vs hH_4R pEC_{50} = 8.5 ± 0.2) with full agonism

on hH$_4$R (α = 1.1 ± 0.1) in a CRE-luc reporter gene assay. Moreover, **14d** does not

activate the H$_1$R and H$_2$R up to 10 µM (Fig. S3).

Equally encouragingly, the binding affinity of **14d** is increased for mH$_3$R (pK$_i$ = 9.0 ± 0.1)

compared to hH$_3$R, while for mH$_4$R the pK$_i$ value is decreased to 7.8 ± 0.0, thus yielding

a substantial H$_3$R/H$_4$R binding selectivity for mouse receptors. Compound **14d** was also

functionally evaluated as agonist on the mH$_3$R and mH$_4$R using the CRE-luciferase

reporter gene assay. In these experiments **14d** displays a 10-fold selectivity in potency

(mH$_3$R pEC$_{50}$ = 10.0 ± 0.1 versus mH$_4$R pEC$_{50}$ = 9.0 ± 0.1), while acting as a full agonist

on both murine receptors (mH$_3$R α = 1.2 ± 0.1 and mH$_4$R α = 1.1 ± 0.1) (Fig. 5B, C).

The metabolic stability of **14d** was determined *in vitro* by incubation with rodent liver

microsomes (Table 2). The pharmacokinetic properties for mouse (t$_{1/2}$ = 130.8 min; Cl$_{int}$

= 20.7 mL·min^{-1}·kg^{-1}) indicate more than 2 times slower elimination compared to the

reference control verapamil.[48] For rat, this difference between **14d** and verapamil is even

more pronounced.

Table 2. Pharmacokinetic properties of **14d** and reference drug verapamil.

Compound	Rat liver microsomes		Mouse liver microsomes	
	$t_{1/2}$ (min)	Cl_{int} (mL·min^{-1}·kg^{-1})	$t_{1/2}$ (min)	Cl_{int} (mL·min^{-1}·kg^{-1})
14d	239.0	7.9	130.8	20.7
Verapamil	50.9	37.3	57.3	47.3

The imidazole ring is known to generally be able to interact with CYP enzymes via coordination of the imidazole with the prosthetic haem iron, which can cause unwanted drug-drug interaction.[49] Since the 2-amino-pyrimidine core contains a pattern of adjacent nitrogen atoms, we measured its propensity for CYP inhibition. Compound **14d** shows only weak activity on three key CYP enzymes (Fig. S4) with IC_{50} values for binding to CYP3A4, CYP2C9 and CYP2D6 all being larger than 25 μM.

Effect of 14d on social recognition in mice.

Given the notion that CNS penetration of H_3R agonists,[1,5] including **14d** is not evident,

we evaluated the *in vivo* CNS effects of **14d** in a standard paradigm for H_3R action. It is

well known that histamine, acting in different brain sites, is an important regulator of

memory consolidation and retrieval in various learning paradigms, including the social

recognition test.[50, 51] We used this behavioral paradigm to investigate the H_3R-related

CNS activity of compound **14d** *in vivo*. The social recognition memory investigates the

ability to remember the identity of a conspecific, that is crucial to the building of social

relationships and survival. Twenty-four hours after animals' habituation to the apparatus,

the subject mouse was placed in an open field arena with an empty cage and another

one containing a juvenile mouse. Mice tend to spend more time in the proximity of the

cage containing the juvenile mouse than the empty one, offering an indication of

sociability. One hour later, the experimental mouse was placed again in the same arena,

but this time one cage contained the familiar mouse and the second one a novel juvenile

mouse. The exploration time of the familiar and the novel mouse were recorded

separately. Compound **14d** at a dose of 5mg/kg or vehicle were given intraperitoneally

(i.p.) 30 min before the training session (Fig. 6A). Compound **14d** did not affect animals'

sociability as revealed by the longer time that they spent exploring the cage containing

the social stimulus compared to the empty cage (Fig. S5). In this respect, mice treated

with compound **14d** behaved like controls. During the test session, control mice

recognized the familiar juvenile, since they spent more time exploring the novel one.

Conversely, mice treated with **14d** did not discriminate between the novel and the familiar

mouse (Fig. 6B). This result clearly suggests a social memory impairment, further

confirmed by the negative discrimination index calculated for the group of animals

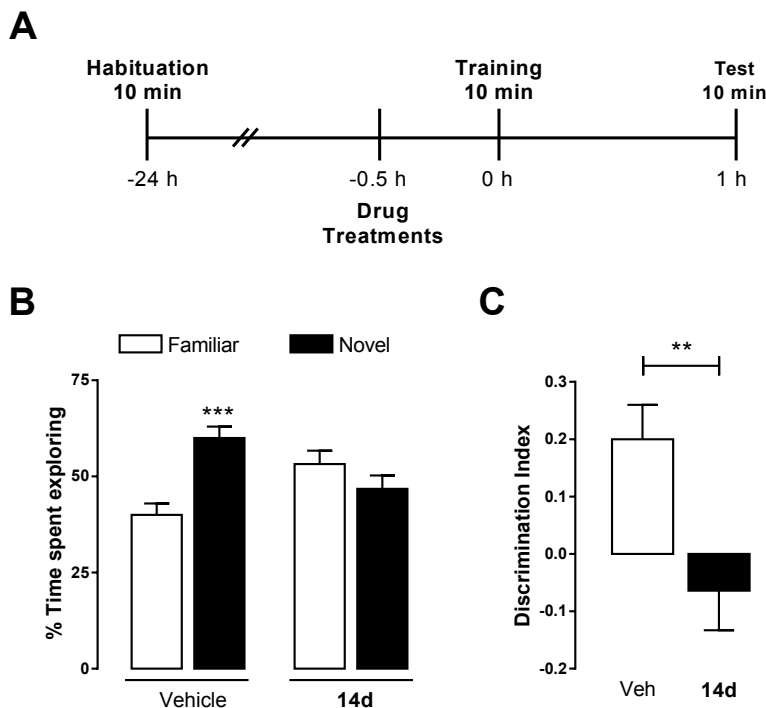receiving injections of **14d** (Fig. 6C).

Figure 6. Compound **14d** impairs social recognition in mice. **A**) Schematic drawings showing the sequence of procedures and treatment administrations. **B**) Results are calculated as means of individual percentage of time spent exploring familiar (white columns) and novel (black columns) social stimuli. ***P<0.001 vs. respective familiar subject (Two-way ANOVA and Bonferroni's MCT). **C**) Discrimination index calculated according to the formula tN-tF/tN+tF. **P<0.01 vs. vehicle (unpaired t-test). Shown are means ± S.E.M. of 10-11 animals per experimental group.

DISCUSSION AND CONCLUSIONS

We present 2-aminopyrimidine derivatives with an alkylated 3-amino-azetidine moiety

showing low nanomolar affinities for the H_3R. Based on the non-imidazole partial agonist

11b identified as an in-house hit, a 23-membered compound set was synthesized and

tested on H_3R. The reduction of the substituent size at position 6 of the pyrimidine ring

(R^1) improved both affinity (pK_i) and potency (pEC_{50}) on hH_3R. Each member of the

extended R^1=H series (**14**) shows full agonism in a CRE-luciferase reporter gene assay,

with three derivatives (**14b**, **c**, **d**) improving upon the endogenous ligand histamine,

combining full H_3R agonism with high (sub)nanomolar potencies. Most notably, the key

non-imidazole H_3R agonist **14d** (VUF16839) combines high affinity for the H_3R (pK_i = 8.5)

with full agonism at the H_3R and a subnanomolar potency (pEC_{50} = 9.5) in a CRE-

luciferase reporter gene assay. However, **14d** acts as a partial agonist in a [35S]GTPγS

accumulation assay with a 13-fold lower potency as compared to the more downstream

CRE-luciferase reporter gene assay, which is most likely the consequence of signal

amplification as suggested by a 25-fold higher potency of the full agonist histamine in the

CRE-luciferase reporter gene assay as compared to a [35S]GTPγS accumulation assay.

From the recent development of numerous series of H_4R antagonists it is known that the 2-aminopyrimidine is a privileged scaffold for H_4R antagonism.[35] As such, it is not surprising that **14d** also binds with relatively high affinity to the H_4R (pK_i = 8.1). It acts as agonist at H_4R, but is 10-fold less potent than at the H_3R, while **14d** is not active at the H_1R and H_2R.

The subnanomolar potency of the non-imidazole compound **14d** as agonist at H_3R is remarkable, as so far only a few low-potency and/or complex non-imidazole ligands have been reported as agonists at H_3R.[27–32] Indeed, replacements of the imidazole ring while maintaining agonism have so far yielded little success. To illustrate, several imbutamine (**2**) analogues in which the imidazole moiety was replaced with an aminopyrimidine, aminopyridine or aminotriazole ring studied were not effective as H_3R agonists.[34] Comparing the activities of the aminopyrimidine analog of **2** with **14d**, the effective activation of H_3R by **14d** suggests a very important role of its azetidine sidechain. Molecular docking combined with MD studies affords a predicted binding mode (Fig. 4) in which **14d** interacts with the same key amino acids (D114[3.32], E206[5.461], Y374[6.51]) as histamine (**1**) (Fig. 4E), suggesting that the 2-aminopyrimidine moiety mimics the

imidazole ring. The computational studies also suggest that the azetidine sidechain

makes an ionic interaction with the same amino acid (D114$^{3.32}$) as the amine group in the

ethylamine sidechain of histamine. Clearly, both **14d** and histamine are able to interact

with the same key amino acids of H$_3$R, despite the fact that the binding modes of **14d** and

histamine do not substantially overlap.

The alkyl substitution of the basic amino moiety of **2** was studied previously in our

group[18] and subtle differences in alkyl substituents on the basic amine strongly influence

the functional activity of such imbutamine analogs. Based on this SAR, we hypothesize

that the basic amine of the 2-aminopyrimidine compound series **11**-**14** might be a

functional „hot spot" as well. In case of the R^1 = *i*Pr series (**11**), this appears to partially

pan out as the chain elongation and dialkylation show moderate drops in intrinsic activity

(α) (compare **11b** vs **11c** and **11i** in Table 1). However, such a trend was not observed

within the other series **12**-**14** (Table 1, Fig. 3D).

The analysis of additional properties for key compound **14d** underscores its suitability

for *in vivo* characterization in mice. That is, mouse potency data (mH$_3$R: pEC$_{50}$ = 10.0,

mH$_4$R: pEC$_{50}$ = 9.0) and *in vitro* elimination parameters in mouse (t$_{1/2}$ = 130.8 min; Cl$_{int}$ =

20.7 mL·min^{-1}·kg^{-1}) all bode well. The inhibition of CYP enzymes is a general issue of

imidazole-containing ligands.[49] Although the diaminopyrimidine core might conceivably

also be prone to the CYP inhibition, **14d** only weakly (IC$_{50}$ > 25 μM) interacts with selected

key CYP enzymes (CYP3A4, CYP2D6, CYP 2C9).

Poor brain penetration is a known problem of some imidazole-containing ligands,[5]

limiting their potential administration routes in CNS-related experiments. As indicated by

the effects in the *in vivo* social memory test, the 2-aminopyrimidine **14d** (5 mg/kg i.p.) is

clearly penetrating the CNS. Histamine is a known modulator of different types of

memory.[3,52] H$_3$R antagonists, such as thioperamide, improve short-term memory, while

H$_3$R agonists such as immepip (**4**) cause amnesia in the social recognition test.[51] The

results shown here confirm and expand these observations, since a memory impairment

was observed also for systemic treatment with compound **14d** in the same paradigm (Fig.

6). It should be noted that H$_3$R activation affects the circadian rhythm by increasing slow

wave sleep and dose-dependently attenuates ciproxifan-induced waking effects.[53] Also,

H$_3$R agonists reduce stress-induced behavior in pre-clinical models.[54] These

observations suggest that H$_3$R activation may affect exploratory activity, which could

negatively impact arousal and cognition. We did not specifically measure **14d**-induced

alterations of sleep-wake cycle; however, **14d**-associated social memory impairment

does not seem to be related to sedative effects, as there were no statistically significant

differences between the control group and **14d** treated mice in exploration time of the

cage in the presence or absence of the social stimulus (during training: vehicle = 144.0 ±

60.0 s; **14d** = 136.2 ± 44.1 s; during test: vehicle = 150.5 ± 42.4 s; **14d** = 148.3 ± 69.4 s).

Moreover, based on the mH_3R/mH_4R selectivity profile of **14d** (*vide supra*), available

literature on H_4R expression, H_4R agonist actions in the CNS, and the behavioral profile

of H_4R-deficient mice excluding a relevant role of this receptor on the histaminergic

modulation of memory processing, it is highly unlikely that the *in vivo* amnesic effects of

14d are confounded by its H_4R activity.[55,56] Indeed, the amnesic effects of **14d** are

consistent with the memory impairments observed following treatment with different H_3R

agonists (imetit (**3**) and *R*-α-methylhistamine) in the object recognition and passive

avoidance tests in rats.[57]

 Concluding, in this study 2-aminopyrimidine derivatives with an alkylated 3-amino-

azetidine side chain are presented as highly potent, non-imidazole agonists for the H_3R.

The key *n*-propyl derivative (**14d**, VUF16839) shows attractive *in vitro* pharmacological properties on human H_3R (pK_i = 8.5, pEC_{50} = 9.5, $\alpha \geq$ 1.0 in a CRE-luciferase reporter gene assay with a 10-fold lower potency at H_4R) and mouse H_3R (pK_i= 9.0, pEC_{50}=10.0, with a >10-fold lower potency at mH_4R). It exerts reasonable metabolic stability in rodent liver microsomes and weak activity on CYP enzymes. Moreover, **14d** causes amnesic effects in a social recognition tests in mice at 5 mg/kg, which is in line with the reported memory loss after administration of other H_3R agonists.[51,57] The observed *in vivo* H_3R effects also indicates appreciable brain penetration of **14d**. Compound **14d** can serve as a useful tool compound for fundamental studies concerning the H_3R, given its excellent affinity and potency, H_3R agonism, and effective brain penetration.

EXPERIMENTAL SECTION

Pharmacology and ADME

Materials. [^{3}H]NAMH (specific activity: 79.7 Ci/mmol) and [^{3}H]histamine (specific activity:17.5 Ci/mmol) was purchased from Perkin Elmer (Groningen, the Netherlands). Human embryonic kidney 293T cells (HEK293T cells) were obtained from ATCC. Ketoconazole, quinidine, sulfaphenazole and verapamil were obtained from Sigma-Aldrich (St. Louis, MO, USA).

Cell culture and transfection. HEK293T cells were cultured in Dulbecco's modified Eagles Medium (DMEM) supplemented with 10 % fetal bovine serum (FBS) and 1 % penicillin and 1 % streptomycin. Two million cells per 10 cm^2 dishes were plated 24 h prior to transfection. Cells were transfected using the PEI method.[58] For radioligand displacement assays, HEK293T cells were transfected with 2500 ng cDNA encoding the hH$_3$R [genbank: AF140538], mH$_3$R [genbank: NM_133849.3], hH$_4$R [genbank: AY136745] or mH$_4$R [genbank: NM_153087.2] and 2500 ng empty plasmid pcDEF3. The

DNA:PEI mixture (ratio 1:4) was incubated for 20 minutes at 22 °C before addition to the cells.

Preparation of cell homogenates. Cell homogenates expressing the hH_3R were harvested 48 h after transfection as reported previously.[59]

Radioligand displacement assays. [³H]NAMH and [³H]histamine displacement assays were performed in binding buffer (50 mM Tris-HCl pH 7.4, 25 °C) by co-incubation of 2 nM [³H]NAMH or 10 nM [³H]histamine, increasing concentrations of unlabelled ligand and cell homogenates expressing the hH_3R or mH_3R or hH_4R, respectively. For mH_4R displacement, similar studies were performed but with 30 nM [³H]histamine. The assay mixture was incubated for 2 hours at 25 °C before rapid filtration over a 0.5 % PEI-coated GF/C filter with a Perkin Elmer filtermate harvester. The filter plate was dried and 300 minutes after 25 µL Microsint O was added, filter bound radioactivity was measured with a Microbeta scintillation counter (Perkin Elmer).

[³⁵S]GTPγS accumulation assay. [³⁵S]GTPγS accumulation experiments on hH_3R were performed as described previously.[60]

Reporter gene assay. HEK293T cells were transfected in suspension with cDNA encoding hH$_3$R, mH$_3$R, hH$_4$R, mH$_4$R, H$_1$R (1000 ng) or H$_2$R (2500 ng), CRE-luciferase (2500 ng) or, NFAT-luciferase (2000 ng) for H$_1$R, and empty pcDEF3 plasmid and 50.000 cells per well were plated on a poly-L-lysine coated white 96 wells plate and grown for an additional 24 hours. Cells were stimulated with increasing ligand concentrations, for H$_3$R and H$_4$R in the presence of 1 μM forskolin at 37 °C and 5 % CO$_2$. After 6 hours medium was aspirated and 25 μL luciferase assay reagent (0.83 mM ATP, 0.83 mM d-luciferin, 18.7 mM MgCl$_2$, 0.78 μM Na$_2$PO$_4$, 38.9 mM Tris-HCl (pH 7.8), 0.39 % glycerol, 0.03 % Triton-X-100, and 2.6 μM dithiothreitol) was added to each well. After 30 minutes of incubation at 37 °C, luminescence was measured with a Mithras plate reader (Berthold, Germany).

Data analysis. Data were analyzed using Graphpad prism 7.02 (Graphpad Software Inc, San Diego, USA). Shown data are mean ± S.E.M. of three individual experiments performed in triplicate unless stated otherwise. Competition binding curves were fitted to a one-site binding model. Obtained IC$_{50}$ values were converted into pK$_i$ values using the Cheng-Prusoff equation.[61] Dose-response curves were fitted using Non-linear regression.

1
2
3
4
5
6
7
8
9
10
11
12
13
14
15
16
17
18
19
20
21
22
23
24
25
26
27
28
29
30
31
32
33
34
35
36
37
38
39
40
41
42
43
44
45
46
47
48
49
50
51
52
53
54
55
56
57
58
59
60

Metabolic stability. The pharmacokinetic parameters of **14d** and the reference drug

verapamil were estimated by using rat (RLMs) or mouse liver microsomes (MLMs)

obtained from Sigma-Aldrich (St. Louis, MO, USA). The tested compounds (50 μM) were

incubated in the presence of microsomes (1 mg/mL) for 5, 15, 30 and 45 min in 10 mM

Tris–HCl buffer (pH = 7.4) at 37 °C. Cold methanol with an internal standard (IS) was

added to terminate each reaction. Next, the reaction mixtures were centrifuged at 14,500

r.p.m. The disappearance of tested compounds in time was calculated by UPLC/MS

Waters ACQUITY™ TQD system with a TQ Detector (Waters, Milford, USA). The course

of the reaction was followed by using the analyte/IS peak height ratio values. For the

determination of $t_{1/2}$ value the slope of linear regression from log concentration remaining

versus time relationships (-k) was used according to Obach[48] (equation 1):

$$t_{1/2} = \frac{-0.683}{k}$$

Conversion of $t_{1/2}$ to intrinsic clearance Cl_{int} (in units of ml/min/kg) was done by using

equation 2:

$$Cl_{int} = \frac{0.693}{t_{1/2}} \times \frac{ml\ incubation}{mg\ microsomes} \times \frac{mg\ microsomes}{gm\ liver} \times \frac{gm\ liver}{kg\ b.w.}$$

where 45 mg of microsomal protein per gram of liver tissue (gm liver) and 87 g of gm

liver per kilogram of body weight (kg b.w.) were applied to calculate Cl_{int} in mice, whereas

61 mg of microsomal protein per gm liver and 45 gm liver per kg b.w. were applied to

calculate Cl_{int} in rats, according to Huang *et al.*[62] and Smith *et al.*[63]

Effect on CYP. Luminescent CYP3A4, CYP2D6 and CYP2C9 P450-Glo™ assays and

protocols were obtained from Promega® (Madison, WI, USA). Compound **14d** was tested

in triplicate at the final concentrations in range from 0.01 to 25 µM. The luminescent signal

was measured by using a microplate reader EnSpire PerkinElmer (Waltham, MA, USA).

Social Recognition Test. Male C57Bl6 mice (8-9 weeks old) behaviour was assessed

in a test apparatus comprising an open-field plexiglass arena (45 x 25 cm and 20 cm high)

placed in a sound attenuated room. The assay paradigm comprises three sessions. On

the first session, mice were placed in the arena containing two empty pencil-wire cups

placed in opposing sides and left free to explore for 10 min. Twenty four hours after this

session, a juvenile mouse (stimulus, 4-5 weeks old), which had no prior contact with the

subject mice, was placed under one of the wire cups while the other cup remained empty.

The subject mouse was then placed in the arena and was allowed free to explore for 10

min. During the third session, performed 1 h later, the same stimulus animal was again

placed under the wire cup and a novel unfamiliar juvenile mouse was placed under the

opposing cup. Subject mice were then placed again in the arena and tested for

discrimination between novel and familiar mice in a 10 min session. Each mouse was

subjected to the procedure separately and care was taken to remove any olfactory/taste

cues by cleaning carefully the arena and wire cups between trials. The position of the

social stimuli (empty x social; familiar x novel) were counterbalanced across subjects and

trials to prevent bias from place preference. Stimulus mice were habituated to remain

under the wire cups several days before behavioural testing. Vehicle or **14d** (5 mg/kg)

were injected systemically (i.p.) 30 min before the second session. The animal's

behaviour during all sessions was videotaped and the time spent actively exploring the

stimuli was analyzed by experienced observers unaware of the experimental groups.

Exploration was defined direct snout-to-cup contact and the time spend climbing on the

cups was not considered. Data are expressed as a percentage of time spent exploring

each cup (social x non-social during the second session or familiar x novel during the

third session) and statistical significance was determined by the two-way ANOVA

followed by Bonferroni's test. We also determined a sociability index (SI), calculated

according to the formula (time exploring social cup (tS) – time exploring non-social cup

(tNS)) / (total exploration time (tS+tNS)) and a discrimination index (DI) was calculated

according to the formula (time exploring the novel mouse (tN) – time exploring the familiar

mouse (tS)) / (total exploration time (tN+tF)) both analyzed using unpaired t-test.

Computational studies

Residue numbering. Residue numbering is displayed throughout the manuscript as

absolute sequence numbers and with generic numbering from GPCRdb[64] also in

superscript, in which the first number denotes the helix, 1–8, the second the residue

position relative to the most-conserved residue, defined as number 50, in a gapped

sequence alignment.

Homology Modelling. A three-dimensional model of the H_3R was constructed on

Modeller v.9.15[65] based on the crystal structure of H_1R (PDB ID: 3RZE).[46] The sequence

of H₃R was obtained from UniProt[66] and aligned to the crystal structure sequence based

on the structure-based alignment of GPCRdb. An optimal structure was selected based

on its ability to retrospectively discriminate between known H₃R fragment-like ligands and

true inactives as described elsewhere.[40]

Docking. A conformational library of all the compounds was obtained with Corina

v3.49[67] and protonated in ChemAxon Calculator (Cxcalc).[68] The most energetically

favorable conformations were docked using PLANTS v1.1.[69] 100 docking poses were

generated per conformation and post-processed with interaction fingerprints (IFPs)

inferred from OpenEye's OChem 1.3 library.[70,71] IFPs are bit vectors that are switched off

(0) or on (1) depending on the occurrence of predefined intermolecular interactions

(apolar, face to face and face to edge aromatic interactions, hydrogen bonds (acceptor

or donor) and ionic interactions (cationic or anionic).

Molecular Dynamics Simulations and Analysis. Ligands were parametrized using the

AM1-BCC charges in Antechamber.[72] The selected models were energy minimized to

optimize protein-ligand interactions and used to run membrane-embedded MD

simulations in GROMACS.[73] Each system was simulated for 100ns after an equilibration

of 5ns with the parameters and conditions described elsewhere.[74] Potential energy,

RMSD, RMSF, and dihedrals of the simulations were analyzed with GROMACS tools,

and residue interactions were analyzed with IFPs.

Nephelometry

In transparent flat-bottom 96-well plates, **14d** was placed at different concentrations in

triplicate (10^{-1} M, $10^{-1.5}$ M, 10^{-2} M, $10^{-2.5}$ M, 10^{-3} M, $10^{-3.5}$ M, 10^{-4} M and $10^{-4.5}$ M) in Tris-

HCl binding buffer (50 mM Tris-HCl, pH 7.4) at least 1 h before the measurement. A

Kaolin dispersion was used as a positive control[75] in each plate at different concentrations

($10^{-2.5}$ M, 10^{-3} M, $10^{-3.5}$ M, 10^{-4} M, $10^{-4.5}$ M, 10^{-5} M and $10^{-5.5}$ M) under the same conditions

as with compound **14d**. Nephelometry measurements were performed with a NEPHELO

star Plus (BMG Labtech, Germany) with the following settings: 1 cycle, measurement

start time 0.1 s, measurement interval time 0.1 s, laser intensity 80%, beam focus 2.0

mm, orbital shaking mode at 200 rpm with an additional shaking time of 10 s before each

cycle. Results were analysed using Matlab R2014A (8.3.0.532) software, plotting all

available data points and plotting mean and standard deviation values in a line chart

compared to Kaolin control. The linear fit (R^2) of the Kaolin control was above 0.985 in all

cases.

Chemistry

General Information. Chemicals and solvents were obtained from commercial suppliers

and were used without further purification. THF was dried by passing through the

PureSolv solvent purification system by Inert®. All reactions were carried out under an

inert N_2 atmosphere. Hydrogenation experiments were performed with routine batch

technology or the H-cube Mini Plus flow reactor. Microwave reactions were performed

with the Biotage Initiator microwave system. TLC analyses were performed with Merck

F254 alumina silica plates using UV visualization or staining. Column purifications were

carried out automatically using Biotage Isolera or Teledyne Isco CombiFlash equipment

using Silicycle Ultra Pure silica gel. Melting point (Mp) for final compounds was

determined using a Büchi M-565 melting point apparatus with a rate of 1 ℃/min. NMR

spectra were recorded on a Bruker 250, 300, 500 or 600 MHz spectrometer. Chemical

shifts are reported in ppm (δ), and the residual solvent was used as internal standard (δ

^{1}H NMR: CDCl$_3$ 7.26; CD$_3$OD 4.87; D$_2$O 4.79; ^{13}C NMR: CDCl$_3$ 77.16; CD$_3$OD 49.00).

Data are reported as follows: chemical shift, multiplicity (s = singlet, d = doublet, t = triplet,

q = quartet, p = pentet, sext = sextet, hept = heptet, br = broad signal, m = multiplet, app

= apparent), coupling constant(s) (Hz) and integration. HRMS spectra were recorded on

Bruker microTOF mass spectrometer using ESI in positive ion mode. Analytical HPLC-

MS analyses were conducted using a Shimadzu LC-20AD liquid chromatograph pump

system connected to a Shimadzu SPDM20A diode array detector with MS detection using

a Shimadzu HPLC-MS 2010EV mass spectrometer. The column used is an Xbridge C18

5 mm column (50mm × 4.6 mm). *Acidic mode:* Solvent B (MeCN / 0.1 % formic acid) and

solvent A (water / 0.1 % formic acid), flow rate of 1.0 mL/min with a run time of 8 min. For

compounds which retention time (t$_R$) was less than 1.5 min with acidic solvent system, a

basic solvent system was used. *Basic mode:* Solvent B (MeCN / 10 % buffer), Solvent A

(water / 10 % buffer). The buffer is a 0.4% (w/v) NH$_4$HCO$_3$ solution in water, adjusted to

pH 8.0 with NH$_4$OH. The analysis was conducted using a flow rate of 1.0 mL/min with a

total run time of 8 min. *Gradient settings* (basic and acidic system): start 5% B, linear

gradient to 90% B in 4.5 min, then isocratic for 1.5 min at 90% B, then linear gradient to

5% B in 0.5 min, then isocratic for 1.5 min at 5% B. All compounds (except **14c** and **14f**) have a purity of ≥95% calculated as the percentage peak area of the target compound by UV detection at 254 nm using the analytical HPLC-MS method listed above. Yields reported are not optimized. The compounds described in Table 1 were checked for the presence of PAINS substructures as described by Baell and Holloway,[76] and no PAINS substructures were identified.

4-(3-aminoazetidin-1-yl)-6-isopropylpyrimidin-2-amine (11a). To a solution of carbamate **21a** (351 mg, 1.14 mmol) in MeOH (20 mL) was added aq. HCl (37%, 0.35 mL, 4.23 mmol). The reaction mixture was stirred at rt overnight. The solvents were removed under reduced pressure. The residue was dissolved in DCM/MeOH (10/1, 10 mL). The pH was adjusted to above 10 with NH_3 solution (7N) in MeOH. The suspension was filtered. The solvents were removed under reduced pressure. The crude product was dissolved in hot EtOH (5 mL) and after addition of EtOAc (5 mL) a precipitate formed. The formed solid was collected by filtration, washed and dried *in vacuo*. Purification by flash chromatography (DCM:MeOH:TEA 100:0:0 to 90:9:1) gave the title compound as a white solid (53 mg, 22 %). Mp: 157.0-157.6 ℃. ^{1}H NMR (600 MHz, CD_3OD) δ 5.58 (s, 1H), 4.25

(t, J = 8.1 Hz, 2H), 3.95 – 3.85 (m, 1H), 3.72 (dd, J = 9.0, 5.2 Hz, 2H), 2.64 (hept, J = 7.0

Hz, 1H), 1.21 (d, J = 6.9 Hz, 6H). ^{13}C NMR (151 MHz, CD$_3$OD) δ 175.4, 165.7, 164.0,

89.8, 59.9, 44.1, 36.6, 22.0. HPLC-MS (basic mode): t_R = 2.6 min, purity: >99 %, [M +

H]$^+$: 208. HR-MS [M + H]$^+$ calcd for C$_{10}$H$_{18}$N$_5$$^+$: 208.1557, found 208.1564.

4-isopropyl-6-(3-(methylamino)azetidin-1-yl)pyrimidin-2-amine (11b). To a solution of

carbamate **21b** (96 mg, 0.30 mmol) in DCM (5 mL) was added HCl in dioxane (4N, 1.0

mL, 4.0 mmol). The reaction mixture was stirred for 3 h at rt. The reaction mixture was

diluted with satd. aq. Na$_2$CO$_3$ (10 mL) and extracted with DCM (3 x 5 mL). The combined

organic phases were dried over Na$_2$SO$_4$, filtered and concentrated *in vacuo*. Purification

by flash chromatography (DCM:MeOH:TEA 100:0:0 to 90:9:1) gave the title compound

as a white solid (45 mg, 68 %). Mp: 81.8-82.4 ℃. ^{1}H NMR (500 MHz, CDCl$_3$) δ 5.47 (s,

1H), 5.05 (br, 2H), 4.23 – 4.15 (m, 2H), 3.76 – 3.63 (m, 3H), 2.65 (hept, J = 6.9 Hz, 1H),

2.42 (s, 3H), 1.19 (d, J = 6.9 Hz, 6H). ^{13}C NMR (126 MHz, CDCl$_3$) δ 173.8, 164.4, 162.0,

89.1, 56.7, 50.5, 35.4, 33.3, 21.6. HPLC-MS (basic mode): t_R = 3.1 min, purity: 97.3 %,

[M + H]$^+$: 222. HR-MS [M + H]$^+$ calcd for C$_{11}$H$_{20}$N$_5$$^+$: 222.1713, found 222.1718.

4-(3-(ethylamino)azetidin-1-yl)-6-isopropylpyrimidin-2-amine (11c). To a solution of carbamate **21c** (79 mg, 0.24 mmol) in MeOH (4 mL) was added aq. HCl (37%, 0.19 mL, 2.29 mmol). The reaction mixture was stirred for at rt overnight. The solvents were removed under reduced pressure. The residue was dissolved in DCM/MeOH (4/1, 8 mL). The pH was adjusted to above 10 with NH_3 solution (7N) in MeOH. The inorganic salts were filtered off, washed with DCM/MeOH (4/1, 12 mL). The filtrate was concentrated under reduced pressure. The crude product was dissolved in hot EtOH (1 mL) and after addition of EtOAc (5 mL) a precipitate formed. The formed solid was collected by filtration, washed and dried *in vacuo*. The title compound was obtained as a white solid (25 mg, 45 %). Mp: 226.2-227.3 ℃. ^{1}H NMR (600 MHz, CD_3OD) δ 5.97 (s, 1H), 4.63 (br, 1H), 4.57 (br, 1H), 4.46 (br, 1H), 4.37 (br, 1H), 4.35 – 4.27 (m, 1H), 3.13 (q, J = 7.2 Hz, 2H), 2.87 (hept, J = 6.8 Hz, 1H), 1.38 (t, J = 7.2 Hz, 3H), 1.32 (d, J = 6.9 Hz, 6H). ^{13}C NMR (151 MHz, CD_3OD) δ 164.2, 163.6, 157.0, 91.5, 54.8, 54.4, 48.2, 42.4, 33.3, 20.9, 11.7. HPLC-MS (basic mode): t_R = 3.2 min, purity: >99 %, [M + H]$^+$: 236. HR-MS [M + H]$^+$ calcd for $C_{12}H_{22}N_5^+$: 236.1870, found 236.1868.

4-(3-(dimethylamino)azetidin-1-yl)-6-isopropylpyrimidin-2-amine (11i). A microwave vial charged with amine **17** (248 mg, 1.44 mmol), N,N-dimethylazetidin-3-amine dihydrochloride (250 mg, 1.44 mmol), DIPEA (0.76 mL, 4.33 mmol) and dioxane (10 mL) was heated for 30 min at 150 °C under microwave irradiation. The reaction mixture was diluted with water (20 mL) and extracted with DCM (3 x 20 mL). The combined organic phases were dried over Na_2SO_4, filtered and concentrated *in vacuo*. Purification by flash chromatography (DCM:MeOH:TEA 100:0:0 to 90:9:1) gave the title compound as a white solid (220 mg, 65 %). Mp: 123.6-123.8 °C. ^{1}H NMR (500 MHz, $CDCl_3$) δ 5.49 (s, 1H), 4.87 (br, 2H), 4.04 (t, *J* = 7.8 Hz, 2H), 3.94 – 3.81 (m, 2H), 3.21 (p, *J* = 5.6 Hz, 1H), 2.65 (hept, *J* = 6.8 Hz, 1H), 2.20 (s, 6H), 1.20 (d, *J* = 6.8 Hz, 6H). ^{13}C NMR (126 MHz, $CDCl_3$) δ 174.0, 164.6, 162.1, 89.1, 56.2, 53.9, 41.8, 35.5, 21.7. HPLC-MS (basic mode): t_R = 3.4 min, purity: 97.8 %, [M + H]$^+$: 236. HR-MS [M + H]$^+$ calcd for $C_{12}H_{22}N_5^+$: 236.1870, found 236.1878.

4-(3-aminoazetidin-1-yl)-6-ethylpyrimidin-2-amine (12a). To a solution of carbamate **22a** (250 mg, 0.85 mmol) in MeOH (20 mL) was added aq. HCl (37%, 0.21 mL, 2.54 mmol). The reaction mixture was stirred at rt overnight. The solvents were removed under

reduced pressure. The residue was dissolved in DCM/MeOH (10/1, 40 mL). The pH was

adjusted to above 10 with NH_3 solution (7N) in MeOH. The suspension was filtered. The

solvents were removed under reduced pressure. The crude product was dissolved in hot

EtOH (5 mL) and after addition of EtOAc (15 mL) a precipitate formed. The formed solid

was collected by filtration, washed and dried *in vacuo*. Dissolving in H_2O (5 mL) and

freeze drying gave the title compound as a white fluffy solid (95 mg, 58 %). Mp: 224.7-

225.9 ℃. ^{1}H NMR (600 MHz, CD_3OD) δ 5.83 (s, 1H), 4.51 – 4.37 (m, 2H), 4.16 – 4.02 (m,

3H), 2.50 (q, J = 7.6 Hz, 2H), 1.18 (t, J = 7.6 Hz, 3H). ^{13}C NMR (151 MHz, CD_3OD) δ

164.1, 160.2, 157.4, 92.7, 56.5, 42.6, 27.1, 12.2. HPLC-MS (basic mode): t_R = 2.3 min,

purity: >99 %, [M + H]$^+$: 194. HR-MS [M + H]$^+$ calcd for $C_9H_{16}N_5^+$: 194.1400, found

194.1410.

4-ethyl-6-(3-(methylamino)azetidin-1-yl)pyrimidin-2-amine (12b). To a solution of

carbamate **22b** (450 mg, 1.46 mmol) in MeOH (20 mL) was added aq. HCl (37%, 0.36

mL, 4.35 mmol). The reaction mixture was stirred at rt overnight. The solvents were

removed under reduced pressure. The residue was dissolved in DCM/MeOH (10/1, 20

mL). The pH was adjusted to above 10 with NH_3 solution (7N) in MeOH. The suspension

was filtered. The solvents were removed under reduced pressure. The crude product was

dissolved in hot EtOH (5 mL) and after addition of EtOAc (15 mL) a precipitate formed.

The formed solid was collected by filtration, washed and dried *in vacuo*. Dissolving in H_2O

(5 mL) and freeze drying gave the title compound as a white fluffy solid (150 mg, 50 %).

Mp: 202.8-203.3 ℃. ^1H NMR (600 MHz, CD_3OD) δ 5.89 (s, 1H), 4.51 – 4.39 (m, 2H), 4.11

(dd, *J* = 10.1, 3.5 Hz, 2H), 3.96 (br, 1H), 2.58 (q, *J* = 7.9 Hz, 2H), 2.55 (s, 3H), 1.27 (t, *J*

= 7.6 Hz, 3H). ^{13}C NMR (151 MHz, CD_3OD) δ 164.1, 160.4, 157.6, 92.6, 55.9, 50.4, 32.3,

27.2, 12.2. HPLC-MS (basic mode): t_R = 2.6 min, purity: >99 %, [M + H]$^+$: 208. HR-MS [M

+ H]$^+$ calcd for $C_{10}H_{18}N_5^+$: 208.1557, found 208.1566.

4-ethyl-6-(3-(ethylamino)azetidin-1-yl)pyrimidin-2-amine (12c). To a solution of

carbamate **22c** (117 mg, 0.36 mmol) in MeOH (4 mL) was added aq. HCl (37%, 0.30 mL,

3.62 mmol). The reaction mixture was stirred for at rt overnight. The solvents were

removed under reduced pressure. The residue was dissolved in DCM/MeOH (9/1, 3 mL).

The pH was adjusted to above 10 with NH_3 solution (7N) in MeOH. The inorganic salts

were filtered off, washed with DCM/MeOH (9/1, 8 mL). The filtrate was concentrated

under reduced pressure. The crude product was dissolved in hot EtOH (1.5 mL) and after

addition of EtOAc (7 mL) a precipitate formed. The formed solid was collected by filtration,

washed and dried *in vacuo*. The title compound was obtained as a white solid (8 mg, 10

%). Mp: 236.6-236.9 ℃. ^{1}H NMR (600 MHz, CD$_3$OD) δ 5.99 (s, 1H), 4.60 (br, 2H), 4.48 –

4.26 (m, 3H), 3.13 (q, *J* = 7.3 Hz, 2H), 2.64 (q, *J* = 7.6 Hz, 2H), 1.38 (t, *J* = 7.2 Hz, 3H),

1.31 (t, *J* = 7.6 Hz, 3H). ^{13}C NMR (151 MHz, CD$_3$OD) δ 164.2, 159.8, 157.0, 92.8, 54.8,

54.4, 48.2, 42.4, 26.8, 12.0, 11.7. HPLC-MS (basic mode): t_R = 2.9 min, purity: >99 %, [M

+ H]$^+$: 222. HR-MS [M + H]$^+$ calcd for C$_{11}$H$_{20}$N$_5$$^+$: 222.1713, found 222.1703.

4-(3-(dimethylamino)azetidin-1-yl-6-ethyl)pyrimidin-2-amine (12i). To a solution of

amine **12b** (110 mg, 0.53 mmol) in MeOH (5 mL) was added formaline (37 %, 47 μL, 0.64

mmol) and AcOH (30 μL, 0.53 mmol). After 10 min of stirring at rt, NaBH(OAc)$_3$ (169 mg,

0.80 mmol) was added and the resulting mixture was stirred for 3 h at rt. The reaction

mixture was quenched with 5 M aq. NaOH (2 drops). The solvents were removed under

reduced pressure. The residue was dissolved in DCM/MeOH (4/1, 8 mL). The pH was

adjusted to above 10 with NH$_3$ solution (7N) in MeOH. The inorganic salts were filtered

and washed with DCM/MeOH (4/1, 12 mL). The filtrate was concentrated under reduced

pressure. The crude product was purified by flash chromatography (DCM:MeOH:TEA

100:0:0 to 90:9:1). The selected fractions were collected and the solvents were removed

under reduced pressure. The residue was dissolved in DCM (5 mL) and washed with

satd. aq. Na_2CO_3 (10 mL). The aqueous phase was extracted with DCM (2 x 5 mL). The

combined organic phases were dried over Na_2SO_4, filtered and concentrated in vacuo.

The residue was dissolved in MeOH (10 mL) and washed with c-hexane (20 mL). The c-

hexane layer was extracted with MeOH (2 x 5 mL). The combined MeOH layers were

concentrated *in vacuo* to give the title compound as a white solid (34 mg, 29 %). Mp:

128.7-128.9 °C. ^{1}H NMR (600 MHz, CD$_3$OD) δ 5.63 (s, 1H), 4.15 – 4.05 (m, 2H), 3.85 (dd,

J = 9.0, 5.1 Hz, 2H), 3.30 – 3.23 (m, 1H), 2.43 (q, J = 7.6 Hz, 2H), 2.23 (s, 6H), 1.20 (t, J

= 7.6 Hz, 3H). ^{13}C NMR (151 MHz, CD$_3$OD) δ 171.6, 165.6, 164.0, 91.3, 57.4, 54.7, 41.9,

31.2, 13.4. HPLC-MS (basic mode): t_R = 2.9 min, purity: >99 %, [M + H]$^+$: 222. HR-MS [M

+ H]$^+$ calcd for $C_{11}H_{20}N_5{}^+$: 222.1713, found 222.1705.

4-(3-aminoazetidin-1-yl)-6-methylpyrimidin-2-amine (13a). To a solution of carbamate

23a (723 mg, 2.59 mmol) in MeOH (25 mL) was added aq. HCl (37%, 3.26 mL, 39.4

mmol). The reaction mixture was stirred at rt overnight. The solvents were removed under

reduced pressure. The residue was dissolved in DCM/MeOH (10/1, 40 mL). The pH was

adjusted to above 10 with NH_3 solution (7N) in MeOH. The suspension was filtered. The

solvents were removed under reduced pressure. The crude product was recrystallized

from EtOH. The crystals were collected by filtration, washed and dried *in vacuo*.

Dissolving in H_2O (5 mL) and freeze drying gave the title compound as a white fluffy solid

(189 mg, 43 %). Mp: 204.7-206.5 ℃. ^{1}H NMR (600 MHz, CD_3OD) δ 5.89 (s, 1H), 4.50 –

4.43 (m, 2H), 4.17 – 4.11 (m, 1H), 4.06 (dd, *J* = 10.6, 4.8 Hz, 2H), 2.28 (s, 3H). ^{13}C NMR

(151 MHz, CD_3OD) δ 164.0, 157.8, 155.9, 94.0, 57.4, 43.0, 19.3. HPLC-MS (basic mode):

t_R = 2.0 min, purity: >99 %, $[M + H]^+$: 180. HR-MS $[M + H]^+$ calcd for $C_8H_{14}N_5^+$: 180.1244,

found 180.1244.

4-methyl-6-(3-(methylamino)azetidin-1-yl)pyrimidin-2-amine dihydrochloride (13b). To

a solution of carbamate **23b** (193 mg, 0.66 mmol) in dioxane (2 mL) was added HCl in

dioxane (4 N, 2.0 mL, 8.0 mmol). The reaction mixture was stirred at rt overnight. The

solvents were removed under reduced pressure. The title compound was obtained as an

off-white solid (176 mg, quant.). Mp: 220.1-220.5 ℃. ^{1}H NMR (600 MHz, CD_3OD/D_2O) δ

6.01 (s, 1H), 4.69 – 4.56 (m, 2H), 4.46 – 4.29 (m, 3H), 2.82 (s, 3H), 2.36 (s, 3H). ^{13}C NMR

(151 MHz, CD_3OD/D_2O) δ 163.4, 156.2, 154.8, 94.3, 54.1, 53.7, 49.3, 31.6, 18.8. HPLC-

MS (basic mode): t_R = 2.3 min, purity: >99 %, [M + H]$^+$: 194. HR-MS [M + H]$^+$ calcd for

$C_9H_{16}N_5{}^+$: 194.1400, found 194.1401.

4-(3-(ethylamino)azetidin-1-yl)-6-methylpyrimidin-2-amine (13c). To a solution of

carbamate **23c** (124 mg, 0.40 mmol) in MeOH (4 mL) was added aq. HCl (37%, 0.33 mL,

3.99 mmol). The reaction mixture was stirred for 3 hours at rt. The solvents were removed

under reduced pressure. The residue was dissolved in DCM/MeOH (9/1, 8 mL). The pH

was adjusted to above 10 with NH_3 solution (7N) in MeOH. The inorganic salts were

filtered off and washed with DCM/MeOH (4/1, 12 mL). The filtrate was concentrated under

reduced pressure. The title compound was obtained as a white solid (70 mg, 84 %). Mp:

218.1-219.2 ℃. ^{1}H NMR (600 MHz, CD$_3$OD) δ 5.85 (s, 1H), 4.44 – 4.34 (m, 2H), 4.03 (dd,

J = 10.6, 4.8 Hz, 2H), 3.98 – 3.91 (m, 1H), 2.78 (q, J = 7.2 Hz, 2H), 2.26 (s, 3H), 1.20 (t,

J = 7.2 Hz, 3H). ^{13}C NMR (151 MHz, CD$_3$OD) δ 164.0, 158.2, 156.4, 93.9, 56.6, 48.9,

42.2, 19.6, 13.8. HPLC-MS (basic mode): t_R = 2.7 min, purity: 96.4 %, [M + H]$^+$: 208. HR-

MS [M + H]$^+$ calcd for $C_{10}H_{18}N_5{}^+$: 208.1557, found 208.1549.

4-(3-(dimethylamino)azetidin-1-yl-6-methyl)pyrimidin-2-amine (13i). Free base 4-

methyl-6-(3-(methylamino)azetidin-1-yl)pyrimidin-2-amine (160 mg, 0.83 mmol) was

obtained from **13b** by neutralization with NH_3 solution (7N) in MeOH and filtration of the

inorganic salt, followed by evaporation of the solvent. The residue was dissolved in MeOH

(5 mL). To this was added formaline (37 %, 74 μL, 0.99 mmol) and AcOH (47 μL, 0.83

mmol). After 10 min of stirring at rt, $NaBH(OAc)_3$ (263 mg, 1.24 mmol) was added and the

resulting mixture was stirred for 3 h at rt. The reaction mixture was quenched with 5 M

aq. NaOH (2 drops). The solvents were removed under reduced pressure. The residue

was dissolved in DCM/MeOH (4/1, 8 mL). The pH was adjusted to above 10 with NH_3

solution (7N) in MeOH. The inorganic salts were filtered off and washed with DCM/MeOH

(4/1, 12 mL). The filtrate was concentrated under reduced pressure. The crude product

was purified by flash chromatography (DCM:MeOH:TEA 100:0:0 to 90:9:1). The selected

fractions were collected and the solvents were removed under reduced pressure. The

residue was dissolved in DCM (5 mL) and washed with satd. aq. Na_2CO_3 (10 mL). The

aqueous phase was extracted with DCM (2 x 5 mL). The combined organic phases were

dried over Na_2SO_4, filtered and concentrated *in vacuo*. The residue was dissolved in

MeOH (10 mL) and washed with *c*-hexane (20 mL). The *c*-hexane layer were extracted

with MeOH (2 x 5 mL). The combined MeOH layers were concentrated *in vacuo* to give

the title compound as a white solid (65 mg, 38 %). Mp: 171.5-172.7 ℃. ^{1}H NMR (600

MHz, CD$_3$OD) δ 5.63 (app d, J = 3.2 Hz, 1H), 4.15 – 4.04 (m, 2H), 3.91 – 3.80 (m, 2H),

3.30 – 3.23 (m, 1H), 2.23 (d, J = 2.5 Hz, 6H), 2.16 (s, 3H). ^{13}C NMR (151 MHz, CD$_3$OD)

δ 166.2, 165.5, 163.9, 92.6, 57.4, 54.7, 41.9, 23.3. HPLC-MS (basic mode): t_R = 2.6 min,

purity: >99 %, [M + H]$^+$: 208. HR-MS [M + H]$^+$ calcd for C$_{10}$H$_{18}$N$_5$$^+$: 208.1557, found

208.1550.

4-(3-aminoazetidin-1-yl)pyrimidin-2-amine fumarate (14a). To a solution of carbamate

24a (433 mg, 1.63 mmol) in MeOH (25 mL) was added aq. HCl (37%, 0.74 mL, 8.94

mmol). The reaction mixture was stirred at rt overnight. The solvents were removed under

reduced pressure. The residue was dissolved in DCM/MeOH (4/1, 25 mL). The pH was

adjusted to above 10 with NH$_3$ solution (7N) in MeOH. The suspension was filtered. The

solvents were removed under reduced pressure. The free base (248 mg, 1.50 mmol) was

dissolved in MeOH (4 mL) and fumaric acid (88 mg, 0.75 mmol) in MeOH (1 mL) was

added. The clear solution was concentrated until a suspension formed. The suspension

was cooled overnight at 5 °C. The formed solid was collected by filtration, washed and

dried *in vacuo*. Dissolving in H$_2$O (5 mL) and freeze drying gave the title compound as a

white fluffy solid (134 mg, 37 %). The base to fumaric acid ratio was 1:0.5 based on the

^{1}H NMR peak integration. Mp: 222.7-224.1 °C. ^{1}H NMR (600 MHz, CD$_3$OD/D$_2$O) δ 7.62

(d, J = 7.3 Hz, 1H), 6.45 (s, 1H), 6.01 (d, J = 7.3 Hz, 1H), 4.57 (br, 2H), 4.38 – 4.15 (m,

3H). ^{13}C NMR (151 MHz, CD$_3$OD/D$_2$O) δ 174.7, 162.9, 155.8, 142.4, 136.3, 95.8, 55.4,

54.9, 41.7. HPLC-MS (basic mode): t_R = 1.7 min, purity: 96.1 %, [M + H]$^+$: 166. HR-MS

[M + H]$^+$ calcd for C$_7$H$_{12}$N$_5^+$: 166.1087, found 166.1082.

4-(3-(methylamino)azetidin-1-yl)pyrimidin-2-amine fumarate (14b). To a solution of

carbamate **24b** (501 mg, 1.79 mmol) in MeOH (8 mL) was added aq. HCl (37%, 0.54 mL,

6.52 mmol). The reaction mixture was stirred at rt overnight. The solvents were removed

under reduced pressure. The residue was dissolved in DCM/MeOH (9/1, 25 mL). The pH

was adjusted to above 10 with NH$_3$ solution (7N) in MeOH. The suspension was filtered.

The solvents were removed under reduced pressure. The crude free base (205 mg, 1.13

mmol) was dissolved in MeOH (25 mL) and fumaric acid (131 mg, 1.13 mmol) in MeOH

(10 mL) was added. The clear solution was concentrated until a suspension formed. The

suspension was cooled for 1 h at 5 °C. The formed solid was collected by filtration,

washed and dried *in vacuo*. Dissolving in H$_2$O (5 mL) and freeze drying gave the title

compound as a white fluffy solid (250 mg, 53 %). The base to fumaric acid ratio was 1:0.7

based on the ^{1}H NMR peak integration. Mp: 230.1-230.5 ℃. ^{1}H NMR (600 MHz,

CD_3OD/D_2O) δ 7.64 (d, J = 7.0 Hz, 1H), 6.43 (s, 1H), 5.96 (d, J = 7.1 Hz, 1H), 4.46 (dd, J

= 11.1, 7.6 Hz, 2H), 4.18 (dd, J = 11.2, 4.5 Hz, 2H), 4.13 – 4.06 (m, 1H), 2.62 (s, 3H). ^{13}C

NMR (151 MHz, CD_3OD/D_2O) δ 175.2, 163.3, 157.7, 146.0, 136.5, 95.5, 54.5, 49.5, 31.8.

HPLC-MS (basic mode): t_R = 2.1 min, purity: 95.6 %, [M + H]$^+$: 180. HR-MS [M + H]$^+$ calcd

for $C_8H_{14}N_5^+$: 180.1244, found 180.1238.

4-(3-(ethylamino)azetidin-1-yl)pyrimidin-2-amine fumarate (14c). To a solution of

carbamate **24c** (117 mg, 0.40 mmol) in MeOH (4 mL) was added aq. HCl (37%, 0.30 mL,

3.62 mmol). The reaction mixture was stirred at rt overnight. The solvents were removed

under reduced pressure. The residue was dissolved in DCM/MeOH (9/1, 4 mL). The pH

was adjusted to above 10 with NH_3 solution (7N) in MeOH. The suspension was filtered.

The solvents were removed under reduced pressure. The crude free base (54 mg, 0.28

mmol) was dissolved in MeOH (8 mL) and fumaric acid (32 mg, 0.28 mmol) in MeOH (3

mL) was added. After partial evaporation of MeOH and addition of EtOAc (3 mL), a

precipitate was formed. The suspension was cooled for 3 h at 5 °C. The formed solid was

collected by filtration, washed and dried *in vacuo*. Dissolving in H_2O (5 mL) and freeze

drying gave the title compound as a white fluffy solid (18 mg, 17 %). The base to fumaric

acid ratio was 1:0.6 based on the ^1H NMR peak integration. Mp: 206.8-208.5 ℃. ^1H NMR

(600 MHz, CD_3OD/D_2O) δ 7.76 (d, *J* = 7.3 Hz, 1H), 6.70 (s, 1H), 6.16 (d, *J* = 7.3 Hz, 1H),

4.68 (br, 2H), 4.55 – 4.31 (m, 3H), 3.19 (q, *J* = 7.3 Hz, 2H), 1.41 (t, *J* = 7.3 Hz, 3H). ^{13}C

NMR (151 MHz, CD_3OD/D_2O) δ 171.9, 163.2, 156.0, 142.7, 136.0, 95.7, 54.5, 54.1, 47.7,

42.3, 11.6. HPLC-MS (basic mode): t_R = 2.2 min, purity: 91.8 %, $[M + H]^+$: 194. HR-MS

$[M + H]^+$ calcd for $C_9H_{16}N_5^+$: 194.1400, found 194.1393.

4-(3-(propylamino)azetidin-1-yl)pyrimidin-2-amine fumarate hydrate (14d, VUF16839).

To a solution of carbamate **24d** (1.19 g, 3.87 mmol) in MeOH (20 mL) was added aq. HCl

(37%, 3.2 mL, 38.6 mmol). The reaction mixture was stirred at rt overnight and

subsequently at 50 °C for 30 min. The solvents were removed under reduced pressure.

The residue was dissolved in DCM/MeOH (4/1, 20 mL). The pH was adjusted to above

10 with NH_3 solution (7N) in MeOH. The suspension was filtered. The solvents were

removed under reduced pressure. The crude free base (871 mg, 3.87 mmol) was

dissolved in MeOH (10 mL) and fumaric acid (453 mg, 3.90 mmol) in MeOH (10 mL) was

added. The solvent was removed under reduced pressure and the residue was

recrystallized from EtOH. The suspension was cooled 1 h at 5 °C. The crystals were

filtered, washed with EtOH and dried *in vacuo*. Dissolving in H_2O (20 mL) and freeze

drying gave the title compound as a white fluffy solid (803 mg, 58 %). The base to fumaric

acid ratio was 1:1 based on the ^{1}H NMR peak integration. Mp: 213.8-214.2 ℃. ^{1}H NMR

(500 MHz, D_2O) δ 7.61 (d, *J* = 7.3 Hz, 1H), 6.43 (s, 2H), 5.99 (d, *J* = 7.3 Hz, 1H), 4.56 (br,

2H), 4.40 – 4.19 (m, 3H), 3.06 – 2.92 (m, 2H), 1.68 (sext, *J* = 7.5 Hz, 2H), 0.94 (t, *J* = 7.4

Hz, 3H). ^{13}C NMR (151 MHz, CD_3OD/D_2O) δ 175.2, 162.9, 155.8, 142.7, 136.3, 95.7,

54.4 53.9, 48.4, 47.9, 20.2, 11.1. HPLC-MS (basic mode): t_R = 2.7 min, purity: 97.9 %, [M

+ H]$^+$: 208. HR-MS [M + H]$^+$ calcd for $C_{10}H_{18}N_5^+$: 208.1557, found 208.1566. Anal. calcd

for $C_{10}H_{17}N_5 \cdot C_4H_4O_4 \cdot 1.75H_2O$: C, 47.38; H, 6.96; N, 19.73; O, 25.92; Cl, 0.00. Found: C,

47.07; H, 6.97; N, 19.43; O, 25.60; Cl, < 0.1.

4-(3-(isopropylamino)azetidin-1-yl)pyrimidin-2-amine fumarate (14e). To a solution of

free base **14a** (100 mg, 0.60 mmol) in DCM (4 mL) and MeOH (1 mL) was added acetone

(48 μL, 0.66 mmol) and AcOH (34 μL, 0.60 mmol). After 10 min of stirring at rt,

NaBH(OAc)$_3$ (201 mg, 0.90 mmol) was added and the resulting mixture was stirred at rt

overnight. The reaction mixture was quenched with 5 M aq. NaOH (2 drops). The solvents

were removed under reduced pressure. The residue was purified by column

chromatography (DCM:MeOH:TEA 100:0:0 to 80:18:2). The selected fractions were

collected and the solvents were removed under reduced pressure. The residue was

dissolved in DCM/MeOH (9/1, 10 mL) and washed with satd. aq. Na_2CO_3 solution (10

mL). The aqueous layer was extracted with DCM/MeOH (9/1, 2 x 5 mL). The combined

organic phases were dried over Na_2SO_4, filtered and concentrated *in vacuo*. The free

base (32 mg, 0.154 mmol) was dissolved in MeOH (1 mL) and fumaric acid (18 mg, 0.154

mmol) in MeOH (1 mL) was added. After partial evaporation of MeOH and addition of

EtOAc (5 mL), a precipitate was formed. The suspension was cooled for 1 h at 5 °C. The

formed solid was collected by filtration, washed and dried *in vacuo*. Dissolving in H_2O (5

mL) and freeze drying gave the title compound as a white fluffy solid (42 mg, 22 %). The

base to fumaric acid ratio was 1:1 based on the ^{1}H NMR peak integration. Mp: 219.0-

219.3 °C. ^{1}H NMR (500 MHz, CD_3OD/D_2O) δ 7.76 (d, *J* = 7.1 Hz, 1H), 6.68 – 6.55 (m,

2H), 6.14 – 6.03 (m, 1H), 4.67 – 4.56 (m, 2H), 4.43 – 4.29 (m, 3H), 3.51 – 3.39 (m, 1H),

1.43 – 1.34 (m, 6H). ^{13}C NMR (151 MHz, CD_3OD/D_2O) δ 174.2, 174.0, 163.4, 157.4,

157.1, 144.9, 144.5, 136.7, 95.5, 95.4, 55.3, 55.1, 50.9, 50.6, 46.2, 46.1, 20.0, 19.8

(multiple sets observed). HPLC-MS (basic mode): t_R = 2.7 min, purity: >99 %, $[M + H]^+$:

208. HR-MS $[M + H]^+$ calcd for $C_{10}H_{18}N_5^+$: 208.1557, found 208.1566.

4-(3-(butylamino)azetidin-1-yl)pyrimidin-2-amine fumarate (14f). To a solution of

carbamate **24f** (32 mg, 0.19 mmol) in MeOH (3 mL) was added aq. HCl (37%, 0.158 mL,

1.19 mmol). The reaction mixture was stirred at rt overnight. The solvents were removed

under reduced pressure. The residue was dissolved in DCM/MeOH (4/1, 5 mL). The pH

was adjusted to above 10 with NH_3 solution (7N) in MeOH. The suspension was filtered.

The solvents were removed under reduced pressure. The free base (48 mg, 0.19 mmol)

was dissolved in MeOH (1 mL) and fumaric acid (22 mg, 0.19 mmol) in MeOH (1 mL) was

added. After partial evaporation of MeOH and addition of EtOAc (5 mL), a precipitate

formed. The suspension was cooled for 1 h at 5 °C. The formed solid was collected by

filtration, washed and dried *in vacuo*. The title compound was obtained as a white solid

(34 mg, 58 %). The base to fumaric acid ratio was 1:0.75 based on the ^{1}H NMR peak

integration. Mp: 169.6-169.9 ℃. ^{1}H NMR (600 MHz, CD_3OD/D_2O) δ 7.72 – 7.66 (m, 1H),

6.66 (s, 1H), 6.06 (d, *J* = 7.2 Hz, 1H), 4.54 (br, 2H), 4.34 (br, 2H), 4.27 – 4.21 (m, 1H),

3.02 – 2.95 (m, 2H), 1.72 – 1.64 (m, 2H), 1.43 (sext, J = 7.4 Hz, 2H), 0.97 (t, J = 7.4 Hz,

3H). ^{13}C NMR (151 MHz, CD$_3$OD/D$_2$O) δ 170.0, 163.6, 156.7, 143.1, 135.8, 95.5, 54.7,

48.6, 47.0, 29.6, 20.9, 13.9. HPLC-MS (basic mode): t_R = 3.1 min, purity: 94.6 %, [M +

H]$^+$: 222. HR-MS [M + H]$^+$ calcd for C$_{11}$H$_{20}$N$_5^+$: 222.1713, found 222.1705.

(*rac*)-4-(3-(*sec*-butylamino)azetidin-1-yl)pyrimidin-2-amine fumarate (14g). To a

solution of free base **14a** (100 mg, 0.60 mmol) in DCM (4 mL) and MeOH (1 mL) was

added butane-2-one (64 μL, 0.66 mmol) and AcOH (34 μL, 0.60 mmol). After 10 min of

stirring at rt, NaBH(OAc)$_3$ (201 mg, 0.90 mmol) was added and the resulting mixture was

stirred at rt overnight. The reaction mixture was quenched with 5 M aq. NaOH (2 drops).

The solvents were removed under reduced pressure. The residue was purified by column

chromatography (DCM:MeOH:TEA 100:0:0 to 80:18:2). The selected fractions were

collected and the solvents were removed under reduced pressure. The residue was

dissolved in DCM/MeOH (9/1, 10 mL) and washed with satd. aq. Na$_2$CO$_3$ solution (10

mL). The aqueous layer was extracted with DCM/MeOH (9/1, 2 x 5 mL). The combined

organic phases were dried over Na$_2$SO$_4$, filtered and concentrated *in vacuo*. The free

base (25 mg, 0.113 mmol) was dissolved in MeOH (1 mL) and fumaric acid (13 mg, 0.113

mmol) in MeOH (1 mL) was added. After partial evaporation of MeOH and addition of

EtOAc (5 mL), a precipitate formed. The suspension was cooled for 1 h at 5 °C. The

formed solid was collected by filtration, washed and dried *in vacuo*. Dissolving in H_2O (5

mL) and freeze drying gave the title compound as a white fluffy solid (32 mg, 16 %). The

base to fumaric acid ratio was 1:1 based on the ^{1}H NMR peak integration. Mp: 214.6-

215.4 °C. ^{1}H NMR (500 MHz, CD_3OD/D_2O) δ 7.74 (d, *J* = 7.1 Hz, 1H), 6.64 – 6.53 (m,

2H), 6.12 – 6.05 (m, 1H), 4.62 (br, 2H), 4.47 – 4.30 (m, 3H), 3.28 (br, 1H), 1.90 – 1.80 (m,

1H), 1.69 – 1.57 (m, 1H), 1.38 – 1.30 (m, 3H), 1.05 (t, *J* = 7.5 Hz, 3H). ^{13}C NMR (151

MHz, CD_3OD/D_2O) δ 174.5, 174.1, 163.2, 156.9, 156.8, 144.3, 143.8, 136.7, 95.6, 95.5,

56.1, 56.0, 55.0, 46.1, 46.0, 27.4, 27.2, 16.3, 16.2, 9.8 (multiple sets observed). HPLC-

MS (basic mode): t_R = 3.0 min, purity: 95.6 %, $[M + H]^+$: 222. HR-MS $[M + H]^+$ calcd for

$C_{11}H_{20}N_5^+$: 222.1713, found 222.1715.

4-(3-(isobutylamino)azetidin-1-yl)pyrimidin-2-amine fumarate (14h). To a solution of

free base **14a** (100 mg, 0.60 mmol) in DCM (4 mL) and MeOH (1 mL) was added

isobutyraldehyde (66 μL, 0.66 mmol) and AcOH (34 μL, 0.60 mmol). After 10 min of

stirring at rt, NaBH(OAc)$_3$ (201 mg, 0.90 mmol) was added and the resulting mixture was

stirred at rt overnight. The reaction mixture was quenched with 5 M aq. NaOH (2 drops).

The solvents were removed under reduced pressure. The residue was purified by column

chromatography (DCM:MeOH:TEA 100:0:0 to 80:18:2). The selected fractions were

collected and the solvents were removed under reduced pressure. The residue was

dissolved in DCM/MeOH (9/1, 10 mL) and washed with satd. aq. Na_2CO_3 solution (10

mL). The aqueous layer was extracted with DCM/MeOH (9/1, 2 x 5 mL). The combined

organic phases were dried over Na_2SO_4, filtered and concentrated *in vacuo*. The free

base (59 mg, 0.267 mmol) was dissolved in MeOH (1 mL) and fumaric acid (31 mg, 0.267

mmol) in MeOH (1 mL) was added. After partial evaporation of MeOH and addition of

EtOAc (5 mL), a precipitate formed. The suspension was cooled for 1 h at 5 °C. The

formed solid was collected by filtration, washed and dried *in vacuo*. Dissolving in H_2O (5

mL) and freeze drying gave the title compound as a white fluffy solid (78 mg, 38 %). The

base to fumaric acid ratio was 1:1 based on the ^{1}H NMR peak integration. Mp: 230.9-

231.3 °C. ^{1}H NMR (500 MHz, CD_3OD/D_2O) δ 7.73 (d, *J* = 7.2 Hz, 1H), 6.59 – 6.55 (m,

2H), 6.09 (d, *J* = 7.2 Hz, 1H), 4.59 (t, *J* = 9.5 Hz, 2H), 4.37 (br app d, 2H), 4.30 – 4.23 (m,

1H), 2.88 (dd, *J* = 7.2, 3.6 Hz, 2H), 2.11 – 2.03 (m, 1H), 1.08 (d, *J* = 6.7 Hz, 6H). ^{13}C NMR

(151 MHz, CD$_3$ODD$_2$O) δ 174.3, 174.2, 163.2, 156.7, 156.7, 143.7, 143.7, 136.6, 95.6,

95.5, 54.6, 54.0, 48.6, 27.3, 27.2, 20.3 (multiple sets observed). HPLC-MS (basic mode):

t$_R$ = 3.1 min, purity: >99 %, [M + H]$^+$: 222. HR-MS [M + H]$^+$ calcd for C$_{11}$H$_{20}$N$_5^+$: 222.1713,

found 222.1716.

4-(3-(dimethylamino)azetidin-1-yl)pyrimidin-2-amine fumarate (14i). To a solution of

amine fumarate **14b** (100 mg, 0.34 mmol) in MeOH (25 mL) was added formaline (37 %,

70 μL, 0.94 mmol) and AcOH (20 μL, 0.34 mmol). After 10 min of stirring at rt,

NaBH(OAc)$_3$ (108 mg, 0.68 mmol) was added and the resulting mixture was stirred at rt

overnight. The reaction mixture was quenched with 5 M aq. NaOH (2 drops). The solvents

were removed under reduced pressure. The residue was purified by column

chromatography (DCM:MeOH:TEA 100:0:0 to 90:9:1). The selected fractions were

collected and the solvents were removed under reduced pressure. The residue was

dissolved in DCM/MeOH (9/1, 20 mL). The pH was adjusted to above 10 with NH$_3$ solution

(7N) in MeOH. The suspension was filtered. The solvents were removed under reduced

pressure. The crude free base (25 mg, 0.130 mmol) was dissolved in MeOH (5 mL) and

fumaric acid (7.5 mg, 0.065 mmol) in MeOH (2.5 mL) was added. The solvent was

evaporated until a suspension formed. The suspension was cooled overnight at 5 °C. The

formed solid was collected by filtration, washed and dried *in vacuo*. Dissolving in H_2O (5

mL) and freeze drying gave the title compound as a white fluffy solid (31 mg, 36 %). The

base to fumaric acid ratio was 1:0.5 based on the ^{1}H NMR peak integration. Mp: 224.0-

224.4 °C. ^{1}H NMR (500 MHz, CD_3OD/D_2O) δ 7.66 (d, J = 7.0 Hz, 1H), 6.50 (s, 1H), 5.98

(d, J = 7.0 Hz, 1H), 4.35 – 4.27 (m, 2H), 4.08 (dd, J = 10.8, 4.9 Hz, 2H), 3.62 – 3.53 (m,

1H), 2.36 (s, 6H). ^{13}C NMR (151 MHz, CD_3OD/D_2O) δ 175.0, 163.2, 157.8, 145.6, 136.7,

95.4, 56.4, 54.4, 41.5. HPLC-MS (basic mode): t_R = 2.4 min, purity: >99 %, $[M + H]^+$: 194.

HR-MS $[M + H]^+$ calcd for $C_9H_{16}N_5^+$: 194.1400, found 194.1395.

4-(3-(diethylamino)azetidin-1-yl)pyrimidin-2-amine fumarate (14j). To a solution of free

base **14a** (100 mg, 0.60 mmol) in DCM (4 mL) and MeOH (1 mL) was added acetaldehyde

(0.34 mL, 6 mmol) and AcOH (34 μL, 0.60 mmol). After 10 min of stirring at rt,

NaBH(OAc)$_3$ (402 mg, 1.80 mmol) was added and the resulting mixture was stirred at rt

overnight. The reaction mixture was quenched with 5 M aq. NaOH (2 drops). The solvents

were removed under reduced pressure. The residue was purified by column

chromatography (DCM:MeOH:TEA 100:0:0 to 80:18:2). The selected fractions were

collected and the solvents were removed under reduced pressure. The residue was dissolved in DCM/MeOH (9/1, 10 mL) and washed with satd. aq. Na_2CO_3 solution (10 mL). The aqueous layer was extracted with DCM/MeOH (9/1, 2 x 5 mL). The combined organic phases were dried over Na_2SO_4, filtered and concentrated *in vacuo*. The free base (82 mg, 0.37 mmol) was dissolved in MeOH (1 mL) and fumaric acid (43 mg, 0.37 mmol) in MeOH (1 mL) was added. After partial evaporation of MeOH and addition of EtOAc (5 mL), a precipitate formed. The suspension was cooled for 1 h at 5 °C. The formed solid was collected by filtration, washed and dried *in vacuo*. Dissolving in H_2O (5 mL) and freeze drying gave the title compound as a white fluffy solid (90 mg, 44 %). The base to fumaric acid ratio was 1:1 based on the ^{1}H NMR peak integration. Mp: 229.6-229.8 °C. ^{1}H NMR (600 MHz, CD_3OD/D_2O) δ 7.74 (d, J = 7.1 Hz, 1H), 6.64 – 6.55 (m, 2H), 6.10 (dd, J = 7.2, 4.0 Hz, 1H), 4.62 – 4.51 (m, 2H), 4.50 – 4.41 (m, 2H), 4.41 – 4.29 (m, 1H), 3.28 – 3.13 (m, 4H), 1.40 – 1.27 (m, 6H). ^{13}C NMR (151 MHz, CD_3OD/D_2O) δ 174.1, 173.8, 163.3, 157.0, 156.9, 144.1, 144.0, 136.6, 95.6, 95.5, 53.9, 52.7, 45.6, 45.4, 9.3, 9.2 (multiple sets observed). HPLC-MS (basic mode): t_R = 3.0 min, purity: 97.3 %, [M + H]$^+$: 222. HR-MS [M + H]$^+$ calcd for $C_{11}H_{20}N_5^+$: 222.1713, found 222.1722.

4-(3-(pyrrolidin-1-yl)azetidin-1-yl)pyrimidin-2-amine fumarate (14k). To a solution of free

base **14a** (100 mg, 0.60 mmol) in MeCN (20 mL) were added 1,4-diiodobutane (0.095

mL, 0.72 mmol) and K_2CO_3 (166 mg, 1.20 mmol). The resulting mixture was heated at

reflux for 16 h. The solvent was removed under reduced pressure. The residue was

purified by column chromatography (DCM:MeOH:TEA 100:0:0 to 80:18:2). The selected

fractions were collected and the solvents were removed under reduced pressure. The

residue was dissolved in DCM/MeOH (9/1, 10 mL) and washed with satd. aq. Na_2CO_3

solution (10 mL). The aqueous layer was extracted with DCM/MeOH (9/1, 2 x 5 mL). The

combined organic phases were dried over Na_2SO_4, filtered and concentrated *in vacuo*.

The free base (32 mg, 0.146 mmol) was dissolved in MeOH (1 mL) and fumaric acid (17

mg, 0.146 mmol) in MeOH (1 mL) was added. After partial evaporation of MeOH and

addition of EtOAc (5 mL), a precipitate formed. The suspension was cooled for 1 h at 5

°C. The formed solid was collected by filtration, washed and dried *in vacuo*. Dissolving in

H_2O (5 mL) and freeze drying gave the title compound as a white fluffy solid (20 mg, 9

%). The base to fumaric acid ratio was 1:1.15 based on the ^{1}H NMR peak integration. Mp:

228.3-228.6 ℃. ^{1}H NMR (600 MHz, CD_3OD/D_2O) δ 7.74 (d, *J* = 7.2 Hz, 1H), 6.58 (s, 2H),

6.12 (d, J = 7.2 Hz, 1H), 4.63 (br, 2H), 4.46 (br, 2H), 4.39 – 4.31 (m, 1H), 3.42 (br, 4H),

2.24 – 2.11 (m, 4H). ^{13}C NMR (151 MHz, CD$_3$OD/D$_2$O) δ 173.8, 163.2, 156.3, 143.2,

136.4, 95.6, 54.6, 54.1, 53.3, 24.2. HPLC-MS (basic mode): t_R = 2.8 min, purity: >99 %,

[M + H]$^+$: 220. HR-MS [M + H]$^+$ calcd for C$_{11}$H$_{18}$N$_5$$^+$: 220.1557, found 220.1563.

4-chloro-6-isopropylpyrimidin-2-amine (17). Pyrimidin-4(3H)-one **15** (4.87 g, 31.8

mmol) was dissolved in POCl$_3$ (40 mL, 0.43 mol). The mixture was heated to reflux for 3

h. The solvent was removed under reduced pressure. Ice (150 g) was carefully added to

the residue. The pH of the mixture was adjusted to 9-10 with aq. NaOH (2.5 M). The

mixture was extracted with DCM (3 x 100 mL). The combined organic phases were dried

over Na$_2$SO$_4$, filtered and concentrated *in vacuo*. Purification by flash chromatography

(DCM:MeOH 10:0 to 9:1) gave the title compound as an off-white solid (1.41 g, 26 %). ^{1}H

NMR (500 MHz, CDCl$_3$) δ 6.53 (s, 1H), 5.33 (br, 2H), 2.77 (hept, J = 6.9 Hz, 1H), 1.22 (d,

J = 6.9 Hz, 6H). HPLC-MS (acidic mode): t_R = 3.5 min, purity: 96.8 %, [M + H]$^+$: 172.

4-chloro-6-ethylpyrimidin-2-amine (18). Pyrimidin-4(3H)-one **16** (6.13 g, 44.1 mmol)

was dissolved in POCl$_3$ (50 mL, 0.54 mol). The mixture was heated to reflux for 3 h. The

solvent was removed under reduced pressure. Ice (150 g) was carefully added to the

residue. The pH of the mixture was adjusted to 9-10 with aq. NaOH (2.5 M). The mixture

was extracted with DCM (3 x 10 mL). The combined organic phases were dried over

Na$_2$SO$_4$, filtered and concentrated *in vacuo*. Purification by flash chromatography

(DCM:MeOH 10:0 to 9:1) gave the title compound as an off-white solid (3.63 g, 52 %). ^{1}H

(500 MHz, CDCl$_3$) δ 6.53 (s, 1H), 5.43 (br, 2H), 2.57 (q, *J* = 7.6 Hz, 2H), 1.23 (t, *J* = 7.6

Hz, 3H). HPLC-MS (acidic mode): t$_R$ = 3.0 min, purity: >99 %, [M + H]$^+$: 158.

Tert-butyl   (1-(2-amino-6-isopropylpyrimidin-4-yl)azetidin-3-yl)carbamate   **(21a)**.   A

microwave vial charged with chloride **17** (400 g, 2.33 mmol), carbamate **28a** (402 mg,

2.33 mmol), DIPEA (0.41 mL, 2.33 mmol) and dioxane (10 mL) was heated for 120 min

at 150 °C under microwave irradiation. The reaction mixture was diluted with water (20

mL) and extracted with DCM (3 x 20 mL). The combined organic phases were dried over

Na$_2$SO$_4$, filtered and concentrated *in vacuo*. Purification by flash chromatography

(DCM:MeOH:TEA 100:0:0 to 90:9:1) gave the title compound as a colorless oil (351 mg,

49 %). ^{1}H NMR (300 MHz, CDCl$_3$) δ 5.48 (s, 1H), 5.01 (br, 1H), 4.80 (br, 2H), 4.57 (br,

1H), 4.31 (t, *J* = 8.3 Hz, 2H), 3.89 – 3.74 (m, 2H), 2.65 (hept, *J* = 6.9 Hz, 1H), 1.45 (s, 9H),

1.19 (d, J = 6.9 Hz, 6H). HPLC-MS (acidic mode): t_R = 3.1 min, purity: >99 %, [M + H]+:

308.

Tert-butyl (1-(2-amino-6-isopropylpyrimidin-4-yl)azetidin-3-yl)(methyl)carbamate (21b).

A microwave vial charged with chloride **17** (300 mg, 1.75 mmol), carbamate hydrochloride

28b (389 mg, 1.75 mmol), DIPEA (0.61 mL, 3.50 mmol) and dioxane (10 mL) was heated

for 30 min at 150 °C under microwave irradiation. The reaction mixture was diluted with

water (20 mL) and extracted with DCM (3 x 15 mL). The combined organic phases were

dried over Na_2SO_4, filtered and concentrated *in vacuo*. Purification by flash

chromatography (DCM:MeOH 10:0 to 9:1) gave the title compound as a yellow oil (280

mg, 50 %). ^{1}H NMR (250 MHz, CDCl3) δ 5.50 (s, 1H), 5.03 (br, 1H), 4.79 (br, 2H), 4.20 (t,

J = 8.6 Hz, 2H), 4.07 – 3.95 (m, 2H), 2.93 (s, 3H), 2.65 (hept, J = 6.9 Hz, 1H), 1.46 (s,

9H), 1.20 (d, J = 6.9 Hz, 6H). HPLC-MS (acidic mode): t_R = 3.4 min, purity: >99 %, [M +

H]+: 322.

Tert-butyl (1-(2-amino-6-isopropylpyrimidin-4-yl)azetidin-3-yl)(ethyl)carbamate (21c).

Carbamate **27c** (1.02 g, 2.78 mmol) was dissolved in MeOH/EtOH (10/10 mL) and

reacted with H_2 gas under atmospheric pressure using Pd/C (5%, 0.60 g) overnight at rt.

The mixture was filtered over Celite and the filtrate was concentrated *in vacuo*. The resulting yellowish oil (900 mg, a mixture of intermediate and diphenylmethane) was used in the next step without further purification. A microwave vial charged with chloride **17** (103 mg, 0.60 mmol), crude intermediate (221 mg), DIPEA (0.105 mL, 0.60 mmol) and dioxane (5 mL) was heated for 90 min at 150 °C under microwave irradiation. The reaction mixture was diluted with water (10 mL) and extracted with DCM (3 x 10 mL). The combined organic phases were dried over Na_2SO_4, filtered and concentrated *in vacuo*. Purification by flash chromatography (DCM:MeOH 10:0 to 9:1) gave the title compound as a yellowish oil (79 mg, 35 % over two steps, extrapolated). ^{1}H NMR (300 MHz, CDCl$_3$) δ 6.03 (br, 2H), 5.46 (s, 1H), 5.06 (br, 1H), 4.73 (br, 1H), 4.25 (t, J = 8.7 Hz, 2H), 4.17 – 4.05 (m, 2H), 3.33 (q, J = 7.0 Hz, 2H), 2.76 (hept, J = 6.9 Hz, 1H), 1.46 (s, 9H), 1.23 (d, J = 6.9 Hz, 6H), 1.14 (t, J = 7.0 Hz, 3H). HPLC-MS (acidic mode): t$_R$ = 3.6 min, purity: >99% %, [M + H]$^+$: 336.

Tert-butyl (1-(2-amino-6-ethylpyrimidin-4-yl)azetidin-3-yl)carbamate (**22a**). A microwave vial charged with chloride **18** (500 mg, 3.17 mmol), carbamate **28a** (546 mg, 3.17 mmol), DIPEA (0.55 mL, 3.17 mmol) and dioxane (11 mL) was heated for 45 min at

150 °C under microwave irradiation. The reaction mixture was diluted with water (50 mL) and extracted with DCM (3 x 50 mL). The combined organic phases were dried over Na_2SO_4, filtered and concentrated *in vacuo*. Purification by flash chromatography (DCM:MeOH 10:0 to 9:1) gave the title compound as a colorless oil (250 mg, 27 %). ^{1}H NMR (300 MHz, CDCl$_3$) δ 5.49 (s, 1H), 4.99 (br, 1H), 4.78 (br, 2H), 4.58 (br, 1H), 4.31 (t, *J* = 8.3 Hz, 2H), 3.85 – 3.73 (m, 2H), 2.46 (q, *J* = 7.6 Hz, 2H), 1.45 (s, 9H), 1.20 (t, *J* = 7.6 Hz, 3H). HPLC-MS (acidic mode): t_R = 3.0 min, purity: 94.5 %, [M + H]$^+$: 294.

Tert-butyl (1-(2-amino-6-ethylpyrimidin-4-yl)azetidin-3-yl)(methyl)carbamate (22b). A microwave vial charged with chloride **18** (500 mg, 3.17 mmol), carbamate hydrochloride **28b** (707 mg, 3.17 mmol), DIPEA (1.11 mL, 6.35 mmol) and dioxane (11 mL) was heated for 45 min at 150 °C under microwave irradiation. The reaction mixture was diluted with water (15 mL) and extracted with DCM (3 x 10 mL). The combined organic phases were dried over Na_2SO_4, filtered and concentrated *in vacuo*. Purification by flash chromatography (DCM:MeOH 10:0 to 9:1) gave the title compound as a colorless oil (450 mg, 46 %). ^{1}H NMR (300 MHz, CDCl$_3$) δ 5.52 (s, 1H), 5.00 (br, 1H), 4.77 (br, 2H), 4.20 (t, *J* = 8.6 Hz, 2H), 4.07 – 3.94 (m, 2H), 2.92 (s, 3H), 2.47 (q, *J* = 7.6 Hz, 2H), 1.46 (s, 9H),

1.20 (t, J = 7.6 Hz, 3H). HPLC-MS (acidic mode): t_R = 3.1 min, purity: >99 %, $[M + H]^+$:

308.

Tert-butyl (1-(2-amino-6-ethylpyrimidin-4-yl)azetidin-3-yl)(ethyl)carbamate (22c).

Carbamate **27c** (1.02 g, 2.78 mmol) was dissolved in MeOH/EtOH (10/10 mL) and

reacted with H_2 gas under atmospheric pressure using Pd/C (5%, 0.60 g) overnight at rt.

The mixture was filtered over Celite and the filtrate was concentrated *in vacuo*. The

resulting yellowish oil (900 mg, a mixture of intermediate and diphenylmethane) was used

in the next step without further purification. A microwave vial charged with chloride **18** (95

mg, 0.60 mmol), crude intermediate (221 mg), DIPEA (0.105 mL, 0.60 mmol) and dioxane

(5 mL) was heated for 90 min at 150 °C under microwave irradiation. The reaction mixture

was diluted with water (10 mL) and extracted with DCM (3 x 10 mL). The combined

organic phases were dried over Na_2SO_4, filtered and concentrated *in vacuo*. Purification

by flash chromatography (DCM:MeOH 10:0 to 9:1) gave the title compound as a yellowish

oil (92 mg, 42 % over two steps, extrapolated). ^{1}H NMR (300 MHz, CDCl$_3$) δ 5.54 (s, 1H),

4.83 (br, 3H), 4.24 (t, J = 8.5 Hz, 2H), 4.12 – 3.96 (m, 2H), 3.36 (q, J = 7.1 Hz, 2H), 2.49

(q, J = 7.6 Hz, 2H), 1.48 (s, 9H), 1.29 – 1.11 (m, 6H). HPLC-MS (acidic mode): t_R = 3.3

min, purity: >99% %, $[M + H]^+$: 322.

Tert-butyl (1-(2-amino-6-methylpyrimidin-4-yl)azetidin-3-yl)carbamate (23a). A

microwave vial charged with chloride **19** (1.00 g, 6.97 mmol), carbamate **28a** (1.20 g, 6.97

mmol), DIPEA (1.22 mL, 6.99 mmol) and dioxane (20 mL) was heated for 60 min at 150

°C under microwave irradiation. The reaction mixture was diluted with water (40 mL) and

extracted with DCM (3 x 40 mL). The combined organic phases were dried over Na_2SO_4,

filtered and concentrated *in vacuo*. Purification by flash chromatography (DCM:MeOH

10:0 to 9:1) gave the title compound as a yellowish solid (726 mg, 36 %). ^{1}H NMR (300

MHz, CDCl$_3$) δ 5.50 (s, 1H), 4.99 (br, 1H), 4.78 (br, 2H), 4.58 (br, 1H), 4.30 (t, J = 8.3 Hz,

2H), 3.83 – 3.73 (m, 2H), 2.20 (s, 3H), 1.45 (s, 9H). HPLC-MS (acidic mode): t_R = 2.7 min,

purity: 95.5 %, $[M + H]^+$: 280.

Tert-butyl (1-(2-amino-6-methylpyrimidin-4-yl)azetidin-3-yl)(methyl)carbamate (23b). A

microwave vial charged with chloride **19** (287 mg, 2.00 mmol), carbamate hydrochloride

28b (445 mg, 2.00 mmol), DIPEA (0.70 mL, 4.00 mmol) and dioxane (4 mL) was heated

for 60 min at 150 °C under microwave irradiation. The reaction mixture was diluted with

water (15 mL) and extracted with DCM (3 x 10 mL). The combined organic phases were dried over Na_2SO_4, filtered and concentrated *in vacuo*. Purification by flash chromatography (DCM:MeOH 100:0 to 92:8) gave the title compound as a colorless oil (501 mg, 46 %). ^{1}H NMR (300 MHz, $CDCl_3$) δ 5.51 (s, 1H), 4.99 (br, 1H), 4.81 (br, 2H), 4.19 (t, *J* = 8.6 Hz, 2H), 4.06 – 3.93 (m, 2H), 2.91 (s, 3H), 2.19 (s, 3H), 1.46 (s, 9H). HPLC-MS (acidic mode): t_R = 2.9 min, purity: 95.9 %, $[M + H]^+$: 294.

Tert-butyl (1-(2-amino-6-methylpyrimidin-4-yl)azetidin-3-yl)(ethyl)carbamate (23c). Carbamate **27c** (1.02 g, 2.78 mmol) was dissolved in MeOH/EtOH (10/10 mL) and reacted with H_2 gas under atmospheric pressure using Pd/C (5%, 0.60 g) overnight at rt. The mixture was filtered over Celite and the filtrate was concentrated *in vacuo*. The resulting yellowish oil (900 mg, a mixture of intermediate and diphenylmethane) was used in the next step without further purification. A microwave vial charged with chloride **19** (101 mg, 0.71 mmol), crude intermediate (260 mg), DIPEA (0.123 mL, 0.71 mmol) and dioxane (3 mL) was heated for 90 min at 150 °C under microwave irradiation. The reaction mixture was diluted with water (10 mL) and extracted with DCM (3 x 10 mL). The combined organic phases were dried over Na_2SO_4, filtered and concentrated *in vacuo*.

Purification by flash chromatography (DCM:MeOH 10:0 to 9:1) gave the title compound as a colorless oil (125 mg, 56 % over two steps, extrapolated). ^{1}H NMR (300 MHz, CDCl$_3$) δ 5.52 (s, 1H), 4.75 (br, 3H), 4.20 (t, J = 8.5 Hz, 2H), 4.07 – 3.95 (m, 2H), 3.33 (q, J = 7.0 Hz, 2H), 2.20 (s, 3H), 1.46 (s, 9H), 1.15 (t, J = 7.0 Hz, 3H). HPLC-MS (acidic mode): t$_R$ = 3.2 min, purity: >99% %, [M + H]$^+$: 308.

Tert-butyl (1-(2-aminopyrimidin-4-yl)azetidin-3-yl)carbamate (24a). A microwave vial charged with chloride **20** (500 mg, 3.86 mmol), carbamate **28a** (665 mg, 3.86 mmol), DIPEA (0.67 mL, 3.86 mmol) and dioxane (10 mL) was heated for 60 min at 150 °C under microwave irradiation. The reaction mixture was diluted with water (40 mL) and extracted with DCM (3 x 40 mL). The combined organic phases were dried over Na$_2$SO$_4$, filtered and concentrated *in vacuo*. Purification by flash chromatography (DCM:MeOH 100:0 to 88:12) gave the title compound as a colorless oil (434 mg, 39 %). ^{1}H NMR (300 MHz, CDCl$_3$) δ 7.83 (d, J = 5.8 Hz, 1H), 5.61 (d, J = 5.8 Hz, 1H), 5.10 (br, 1H), 4.82 (s, 2H), 4.58 (br, 1H), 4.31 (t, J = 8.4 Hz, 2H), 3.86 – 3.74 (m, 2H), 1.45 (s, 9H). HPLC-MS (acidic mode): t$_R$ = 2.6 min, purity: 91.6 %, [M + H]$^+$: 266.

Tert-butyl (1-(2-aminopyrimidin-4-yl)azetidin-3-yl)(methyl)carbamate (24b). A microwave vial charged with chloride **20** (500 mg, 3.86 mmol), carbamate hydrochloride **28b** (723 mg, 3.86 mmol), DIPEA (1.35 mL, 7.72 mmol) and dioxane (10 mL) was heated for 30 min at 150 °C under microwave irradiation. The reaction mixture was diluted with water (40 mL) and extracted with DCM (3 x 40 mL). The combined organic phases were dried over Na_2SO_4, filtered and concentrated *in vacuo*. Purification by flash chromatography (DCM:MeOH 100:0 to 88:12) gave the title compound as a colorless oil (501 mg, 46 %). ^1H NMR (300 MHz, $CDCl_3$) δ 7.84 (d, *J* = 5.9 Hz, 1H), 5.65 (d, *J* = 5.9 Hz, 1H), 5.21 – 4.59 (m, 3H), 4.22 (t, *J* = 8.7 Hz, 2H), 4.09 – 3.98 (m, 2H), 2.93 (s, 3H), 1.47 (s, 9H). HPLC-MS (acidic mode): t_R = 2.8 min, purity: >99 %, $[M + H]^+$: 280.

Tert-butyl (1-(2-aminopyrimidin-4-yl)azetidin-3-yl)(ethyl)carbamate (24c). Carbamate **27c** (1.02 g, 2.78 mmol) was dissolved in MeOH/EtOH (10/10 mL) and reacted with H_2 gas under atmospheric pressure using Pd/C (5%, 0.60 g) overnight at rt. The mixture was filtered through Celite. The Celite cake was washed with MeOH (2 x 5 mL) and the combined filtrates were concentrated *in vacuo*. The resulting yellowish oil (900 mg, a mixture of intermediate and diphenylmethane) was used in the next step without further

purification. A microwave vial charged with chloride **20** (78 mg, 0.60 mmol), crude

intermediate (221 mg), DIPEA (0.105 mL, 0.60 mmol) and dioxane (5 mL) was heated for

90 min at 150 °C under microwave irradiation. The reaction mixture was diluted with water

(10 mL) and extracted with DCM (3 x 10 mL). The combined organic phases were dried

over Na_2SO_4, filtered and concentrated *in vacuo*. Purification by flash chromatography

(DCM:MeOH 10:0 to 9:1) gave the title compound as a colorless oil (117 mg, 50 % over

two steps, extrapolated). ^{1}H NMR (300 MHz, $CDCl_3$) δ 7.84 (d, *J* = 5.8 Hz, 1H), 5.64 (d,

J = 5.8 Hz, 1H), 4.77 (br, 3H), 4.22 (t, *J* = 8.5 Hz, 2H), 4.10 – 3.97 (m, 2H), 3.33 (q, *J* =

7.0 Hz, 2H), 1.45 (s, 9H), 1.15 (t, *J* = 7.0 Hz, 3H). HPLC-MS (acidic mode): t_R = 3.0 min,

purity: 95.5 %, $[M + H]^+$: 294.

Tert-butyl (1-(2-aminopyrimidin-4-yl)azetidin-3-yl)(propyl)carbamate (24d). Carbamate

27d (2.09 g, 5.49 mmol) in MeOH (100 mL) was passed through an H-cube fitted with a

Pd/C (10%) catalyst cartridge at a flow rate of 1 mL/min at 60 °C and at 10 atm H_2

pressure. The solvent was removed *in vacuo*. The resulting colorless oil (2.03 g, a mixture

of intermediate and diphenylmethane) was used in the next step without further

purification. A microwave vial charged with chloride **20** (687 mg, 5.31 mmol), crude

intermediate (2.03 g), DIPEA (0.93 mL, 5.27 mmol) and NMP (5 mL) was heated for 30 min at 120 °C under microwave irradiation. The mixture was purified by flash chromatography (DCM:MeOH:TEA 100:0:0 to 90:9:1). The selected fractions were collected and the solvents were removed under reduced pressure. The residue was dissolved in DCM (50 mL) and washed with satd. aq. Na_2CO_3 (80 mL). The aqueous phase was extracted with DCM (2 x 50 mL). The combined organic phases were dried over Na_2SO_4, filtered and concentrated *in vacuo*. The title compound was obtained as a colorless oil (1.19 g, 71 % over two steps). ^{1}H NMR (500 MHz, $CDCl_3$) δ 7.83 (d, J = 5.8 Hz, 1H), 5.64 (d, J = 5.8 Hz, 1H), 5.06 – 4.38 (m, 3H), 4.20 (t, J = 8.5 Hz, 2H), 4.07 (t, J = 7.6 Hz, 2H), 3.22 (t, J = 7.6 Hz, 2H), 1.54 (sext, J = 7.4 Hz, 2H), 1.44 (s, 9H), 0.88 (t, J = 7.4 Hz, 3H). HPLC-MS (acidic mode): t_R = 3.3 min, purity: >99 %, $[M + H]^+$: 308.

Tert-butyl (1-(2-aminopyrimidin-4-yl)azetidin-3-yl)(butyl)carbamate (24f). A solution of carbamate 27f (178 mg, 0.45 mmol) in MeOH (16 mL) was passed through an H-cube fitted with a Pd/C (10%) catalyst cartridge at a flow rate of 1 mL/min at 60 °C and at 10 atm H_2 pressure. The solvent was removed *in vacuo*. The resulting colorless oil (136 mg, a mixture of intermediate and diphenylmethane) was used in the next step without further

purification. A microwave vial charged with chloride **20** (44 mg, 0.34 mmol), crude

intermediate (136 mg), DIPEA (0.060 mL, 0.34 mmol) and NMP (0.5 mL) was heated for

30 min at 120 °C under microwave irradiation. The mixture was purified by flash

chromatography (DCM:MeOH:TEA 100:0:0 to 80:18:2). The title compound was obtained

as an off-white solid (62 mg, 46 % over two steps). ^{1}H NMR (300 MHz, CD$_3$OD) δ 7.71

(d, J = 6.2 Hz, 1H), 5.77 (d, J = 6.0 Hz, 1H), 4.54 (s, 1H), 4.32 – 4.14 (m, 4H), 3.35 – 3.25

(m, 2H), 1.62 – 1.47 (m, 2H), 1.44 (s, 9H), 1.38 – 1.24 (m, 2H), 0.98 – 0.90 (m, 3H). HPLC-

MS (acidic mode): t$_R$ = 3.4 min, purity: 97.5 %, [M + H]$^+$: 322.

Tert-butyl (1-benzhydrylazetidin-3-yl)carbamate (26). To a solution of amine **25** (5.00 g,

21.0 mmol) in THF (40 mL) at 0 °C were added a solution of di-*tert*-butyl dicarbonate

(5.40, 25.2 mmol) in THF (40 mL) and TEA (3.51 mL, 25.2 mmol). The reaction mixture

was warmed to rt and stirred for 2 h. The solvent was evaporated. Purification by flash

chromatography (*c*-hexane:EtOAc:TEA 100:0:0 to 0:95:5) gave the title compound as a

white solid (4.45 g, 63 %). ^{1}H NMR (300 MHz, CDCl$_3$) δ 7.39 (d, J = 7.6 Hz, 4H), 7.32 –

7.22 (m, 4H), 7.22 – 7.12 (m, 2H), 4.87 (br, 1H), 4.30 (br, 2H), 3.53 (t, J = 6.3 Hz, 2H),

2.82 (br, 2H), 1.42 (s, 9H). HPLC-MS (acidic mode): t_R = 3.5 min, purity: 97.5 %, [M + H]$^+$:

339.

Tert-butyl (1-benzhydrylazetidin-3-yl)(ethyl)carbamate (27c). To a solution of

carbamate **26** (3.10 g, 9.2 mmol) in THF (30 mL) at 0 °C, NaH (60%, 0.44 g, 11.0 mmol)

was added. When the evolution of H_2 gas subsided, iodoethane (0.81 mL, 10.1 mmol)

was added dropwise to the reaction mixture. The resulting mixture was stirred overnight

at rt. The reaction mixture was diluted with water (60 mL) and extracted with DCM (3 x 40

mL). The combined organic phases were dried over Na_2SO_4, filtered and concentrated *in

vacuo*. Purification by flash chromatography (*c*-hexane:EtOAc 10:0 to 7:3) gave the title

compound as a white solid (1.95 g, 58 %). ^{1}H NMR (300 MHz, CDCl$_3$) δ 7.48 – 7.35 (m,

4H), 7.32 – 7.23 (m, 4H), 7.23 – 7.12 (m, 2H), 4.34 (br, 2H), 3.51 (br, 2H), 3.27 (q, *J* = 7.1

Hz, 2H), 2.95 (br, 2H), 1.42 (s, 9H), 1.05 (t, *J* = 7.0 Hz, 3H). HPLC-MS (acidic mode): t_R

= 3.9 min, purity: 99.6 %, [M + H]$^+$: 367.

Tert-butyl (1-benzhydrylazetidin-3-yl)(propyl)carbamate (27d). To a solution of

carbamate **26** (4.55 g, 13.2 mmol) in THF (30 mL) at 0 °C, NaH (95%, 0.40 g, 10.5 mmol)

was added. When the evolution of H_2 gas subsided, iodopropane (1.44 mL, 14.7 mmol)

was added dropwise to the reaction mixture. The resulting mixture was stirred overnight

at rt. The reaction mixture was diluted with water (200 mL) and extracted with DCM (3 x

120 mL). The combined organic phases were dried over Na_2SO_4, filtered and

concentrated *in vacuo*. Purification by flash chromatography (*c*-hexane:EtOAc:TEA

100:0:0 to 70:28.5:1.5) gave the title compound as a white solid (2.09 g, 42 %). ^{1}H NMR

(300 MHz, CDCl$_3$) δ 7.46 – 7.35 (m, 4H), 7.33 – 7.23 (m, 4H), 7.23 – 7.14 (m, 2H), 4.33

(s, 2H), 3.50 (t, *J* = 7.2 Hz, 2H), 3.22 – 3.10 (m, 2H), 2.93 (t, *J* = 6.9 Hz, 2H), 1.51 – 1.36

(m, 11H), 0.85 (t, *J* = 7.4 Hz, 3H). HPLC-MS (acidic mode): t_R = 3.9 min, purity: 99.3 %,

$[M + H]^+$: 381.

Tert-butyl (1-benzhydrylazetidin-3-yl)(butyl)carbamate (27f). To a solution of carbamate

26 (552 mg, 1.60 mmol) in THF (50 mL) at 0 °C, NaH (60%, 77 mg, 1.92 mmol) was

added. When the evolution of H_2 gas subsided, iodobutane (0.20 mL, 1.76 mmol) was

added dropwise to the reaction mixture. The resulting mixture was stirred overnight at rt.

The reaction mixture was diluted with water (20 mL) and extracted with DCM (3 x 15 mL).

The combined organic phases were dried over Na_2SO_4, filtered and concentrated *in*

vacuo. Purification by flash chromatography (*c*-hexane:EtOAc:TEA 100:0:0 to 0:95:5)

gave the title compound as a white solid (178 mg, 28 %). ^{1}H NMR (300 MHz, CDCl$_3$) δ

7.46 – 7.36 (m, 4H), 7.32 – 7.23 (m, 4H), 7.23 – 7.14 (m, 2H), 4.33 (br, 2H), 3.59 – 3.35

(m, 2H), 3.26 – 3.12 (m, 2H), 2.93 (br, 2H), 1.50 – 1.34 (m, 11H, overlaps with residual *c*-

hexane), 1.33 – 1.17 (m, 2H), 0.90 (t, *J* = 7.2 Hz, 3H). HPLC-MS (acidic mode): t$_R$ = 4.4

min, purity: 97.8 %, [M + H]$^+$: 395.

AUTHOR INFORMATION

Corresponding Author

*Phone: +31 20 59 87579. E-mail: r.leurs@vu.nl.

Notes

ACKNOWLEDGMENTS

ABBREVIATIONS USED

AEIC, [(1*S*,2*S*)-2-(2-aminoethyl)-1-(1*H*-imidazol-4-yl)cyclopropane; α, intrinsic activity compared to histamine; *c*AMP, cyclic Adenosine Monophosphate; CRE, *c*AMP response element, DCM, dichloromethane; DIPEA, N,N-diisopropylethylamine; FLIPR, Fluorometric Imaging Plate Reader; GPCR, G protein-coupled receptor; gp, guinea pig;

GTPγS, guanosine 5'-O-[gamma-thio]triphosphate; IFP, interaction fingerprint; i.p.,

intraperitoneal; Mp, melting point; MD, molecular dynamics; NAMH, N-α-

Methylhistamine; NMP, N-Methyl-2-pyrrolidone; SAR, structure-activity relationship; satd.

aq., saturated aqueous; S.D., standard deviation; S.E.M., standard error of mean; SFR,

structure-function relationship; rt, room temperature; TEA, triethylamine; THF,

tetrahydrofuran; μW, microwave reaction

SUPPORTING INFORMATION

Nephelometry results of **14d**, best-scored docking poses of **14d**, functional assay on

H$_1$R and H$_2$R, effect of **14d** on CYP3A4, CYP2D6 and CYP2C9 activity, sociability effect

of **14d** in the social recognition test in mice, HPLC-MS chromatogram and spectra of **14d**,

supplementary Movies 1 and 2, and a CSV file containing the molecular formula strings

and associated biochemical data of **1**, **11a-14k**.

REFERENCES

(1)   Panula, P.; Chazot, P. L.; Cowart, M.; Gutzmer, R.; Leurs, R.; Liu, W. L. S.; Stark,

H.; Thurmond, R. L.; Haas, H. L. International Union of Basic and Clinical

Pharmacology. XCVIII. Histamine receptors. *Pharmacol Rev.* **2014**, *64* (1), 1–15.

(2)   Arrang, J. M.; Garbarg, M.; Schwartz, J. C. Auto-inhibition of brain histamine

release mediated by a novel class (H_3) of histamine receptor. *Nature* **1983**, *302*

(5911), 832–837.

(3)   Schlicker, E.; Kathmann, M. Role of the histamine H_3 receptor in the central nervous

system. *Handb. Exp. Pharmacol.* **2017**, *241*, 277–299.

(4)   Stark, H.; Kathmann, M.; Schlicker, E.; Schunack, W.; Schlegel, B.; Sippl, W.

Medicinal chemical and pharmacological aspects of imidazole-containing histamine

H_3 receptor antagonists. *J. Med. Chem.* **2004**, *4* (9), 965–977.

(5)   Ganellin, C. R.; Leurquin, F.; Piripitsi, A.; Arrang, J. M.; Garbarg, M.; Ligneau, X.;

Schunack, W.; Schwartz, J.-C. Synthesis of potent non-imidazole histamine H_3-

receptor antagonists. *Arch. Pharm. (Weinheim).* **1998**, *331* (12), 395–404.

(6)   Celanire, S.; Wijtmans, M.; Talaga, P.; Leurs, R.; de Esch, I. J. P. Keynote review:

Histamine H$_3$ receptor antagonists reach out for the clinic. *Drug Discov. Today*

2005, *10* (23–24), 1613–1627.

(7)   Lebois, E. P.; Jones, C. K.; Lindsley, C. W. The evolution of histamine H$_3$

antagonists/inverse agonists. *Curr. Top. Med. Chem.* **2011**, *11* (6), 648–660.

(8)   Kuhne, S.; Wijtmans, M.; Lim, H. D.; Leurs, R.; de Esch, I. J. P. Several down, a

few to go: histamine H$_3$ receptor ligands making the final push towards the market?

Expert Opin. Investig. Drugs **2011**, *20* (12), 1629–1648.

(9)   Sadek, B.; Łażewska, D.; Hagenow, S.; Kieć-Kononowicz, K.; Stark, H. Histamine

H$_3$R antagonists: from scaffold hopping to clinical candidates. In *Histamine*

Receptors. The Receptors, vol 28. Humana Press, Cham; Blandina, P., Passani,

M., Eds.; Humana Press, Cham, 2016; pp 109–155.

(10) Kollb-Sielecka, M.; Demolis, P.; Emmerich, J.; Markey, G.; Salmonson, T.; Haas,

M. The European Medicines Agency review of pitolisant for treatment of narcolepsy:

summary of the scientific assessment by the Committee for Medicinal Products for

Human Use. *Sleep Med.* **2017**, *33*, 125–129.

(11) Harmony Biosciences LLC.
https://www.harmonybiosciences.com/newsroom/harmony-biosciences-
announces-fda-approval-of-wakix-r-pitolisant-a-first-in/ (accessed Aug 15, 2019).

(12) Kazuta, Y.; Hirano, K.; Natsume, K.; Yamada, S.; Kimura, R.; Matsumoto, S. I.;
Furuichi, K.; Matsuda, A.; Shuto, S. Cyclopropane-based conformational restriction
of histamine. (1*S*,2*S*)-2-(2-aminoethyl)-1-(1*H*-imidazol-4-yl)cyclopropane, a highly
selective agonist for the histamine H3 receptor, having a *cis*-cyclopropane
structure. *J. Med. Chem.* **2003**, *46* (10), 1980–1988.

(13) Kitbunnadaj, R.; Zuiderveld, O. P.; de Esch, I. J. P.; Vollinga, R. C.; Bakker, R.;
Lutz, M.; Spek, A. L.; Cavoy, E.; Deltent, M.-F.; Menge, W. M. P. B.; Timmerman,
H.; Leurs, R. Synthesis and structure−activity relationships of conformationally
constrained histamine H_3 receptor agonists. *J. Med. Chem.* **2003**, *46* (25), 5445–
5457.

(14) Kitbunnadaj, R.; Zuiderveld, O. P.; Christophe, B.; Hulscher, S.; Menge, W. M. P.

B.; Gelens, E.; Snip, E.; Bakker, R. A.; Celanire, S.; Gillard, M.; Talaga, P.; Timmerman, H.; Leurs, R. Identification of 4-(1*H*-Imidazol-4(5)-ylmethyl)pyridine (immethridine) as a novel, potent, and highly selective histamine H3 receptor agonist. *J. Med. Chem.* **2004**, *47* (10), 2414–2417.

(15) Meier, G.; Krause, M.; Hüls, A.; Ligneau, X.; Pertz, H. H.; Arrang, J. M.; Ganellin, C. R.; Schwartz, J. C.; Schunack, W.; Stark, H. 4-(ω-(Alkyloxy)alkyl)-1*H*-imidazole derivatives as histamine H3 receptor antagonists/agonists. *J. Med. Chem.* **2004**, *47* (10), 2678–2687.

(16) Pelloux-Léon, N.; Fkyerat, A.; Piripitsi, A.; Tertiuk, W.; Schunack, W.; Stark, H.; Garbarg, M.; Ligneau, X.; Arrang, J.-M.; Schwartz, J.-C.; Ganellin, C. R. Meta-substituted aryl(thio)ethers as potent partial agonists (or antagonists) for the histamine H_3 receptor lacking a nitrogen atom in the side chain. *J. Med. Chem.* **2004**, *47* (12), 3264–3274.

(17) Kitbunnadaj, R.; Hashimoto, T.; Poli, E.; Zuiderveld, O. P.; Menozzi, A.; Hidaka, R.; de Esch, I. J. P.; Bakker, R. A.; Menge, W. M. P. B.; Yamatodani, A.; Coruzzi, G.;

Timmerman, H.; Leurs, R. *N*-Substituted Piperidinyl Alkyl Imidazoles: Discovery of methimepip as a potent and selective histamine H3 receptor agonist. *J. Med. Chem.* **2005**, *48* (6), 2100–2107.

(18) Govoni, M.; Lim, H. D.; El-Atmioui, D.; Menge, W. M. P. B.; Timmerman, H.; Bakker, R. A.; Leurs, R.; de Esch, I. J. P. A chemical switch for the modulation of the functional activity of higher homologues of histamine on the human histamine H_3 receptor: effect of various substitutions at the primary amino function. *J. Med. Chem.* **2006**, *49* (8), 2549–2557.

(19) Wijtmans, M.; Celanire, S.; Snip, E.; Gillard, M. R.; Gelens, E.; Collart, P. P.; Venhuis, B. J.; Christophe, B.; Hulscher, S.; van der Goot, H.; Lebon, F.; Timmerman, H.; Bakker, R. A.; Lallemand, B. I. L. F.; Leurs, R.; Talaga, P. E.; de Esch, I. J. P. 4-Benzyl-1*H*-imidazoles with oxazoline termini as histamine H3 receptor agonists. *J. Med. Chem.* **2008**, *51* (10), 2944–2953.

(20) Ishikawa, M.; Furuuchi, T.; Yamauchi, M.; Yokoyama, F.; Kakui, N.; Sato, Y. Synthesis and structure-activity relationships of *N*-aryl-piperidine derivatives as

potent (partial) agonists for human histamine H3 receptor. *Bioorganic Med. Chem.*

2010, *18* (14), 5441–5448.

(21) Ishikawa, M.; Shinei, R.; Yokoyama, F.; Yamauchi, M.; Oyama, M.; Okuma, K.;

Nagayama, T.; Kato, K.; Kakui, N.; Sato, Y. Role of hydrophobic substituents on

the terminal nitrogen of histamine in receptor binding and agonist activity:

development of an orally active histamine type 3 receptor agonist and evaluation of

its antistress activity in mice. *J. Med. Chem.* **2010**, *53* (9), 3840–3844.

(22) Ishikawa, M.; Yamauchi, M.; Yokoyama, F.; Kudo, T.; Sato, Y.; Kakui, N.; Kato, K.;

Watanabe, T. Investigation of the histamine H3 receptor binding site. Design and

synthesis of hybrid agonists with a lipophilic side chain. *J. Med. Chem.* **2010**, *53*

(17), 6445–6456.

(23) Cannon, K. E.; Nalwalk, J. W.; Stadel, R.; Ge, P.; Lawson, D.; Silos-Santiago, I.;

Hough, L. B. Activation of spinal histamine H_3 receptors inhibits mechanical

nociception. *Eur. J. Pharmacol.* **2003**, *470* (3), 139–147.

(24) Yoshimoto, R.; Miyamoto, Y.; Shimamura, K.; Ishihara, A.; Takahashi, K.; Kotani,

H.; Chen, A. S.; Chen, H. Y.; MacNeil, D. J.; Kanatani, A.; Tokita, S. Therapeutic potential of histamine H3 receptor agonist for the treatment of obesity and diabetes mellitus. *Proc. Natl. Acad. Sci.* **2006**, *103* (37), 13866–13871.

(25) Reid, A. C.; Brazin, J. A.; Morrey, C.; Silver, R. B.; Levi, R. Targeting Cardiac Mast Cells: Pharmacological modulation of the local renin-angiotensin system. *Curr. Pharm. Des.* **2011**, *17* (34), 3744–3752.

(26) Hashikawa-Hobara, N.; Chan, N. Y.-K.; Levi, R. Histamine 3 receptor activation reduces the expression of neuronal angiotensin II type 1 receptors in the heart. *J. Pharmacol. Exp. Ther.* **2011**, *340* (1), 185–191.

(27) Lim, H. D.; Smits, R. A.; Bakker, R. A.; Dam, C. M. E. van; de Esch, I. J. P.; Leurs, R. Discovery of *S*-(2-Guanidylethyl)-isothiourea (VUF 8430) as a potent nonimidazole histamine H4 receptor agonist. *J. Med. Chem.* **2006**, *49* (23), 6650–6651.

(28) Leurs, R.; Smit, M. J.; Timmerman, H. Molecular aspects of histamine receptors. In *Receptors*; 1995; Vol. 66, pp 413–463.

(29) van der Goot, H.; Eriks, J. C.; Leurs, R.; Timmerman, H. Amselamine, a new selective histamine H_2-receptor agonist. *Bioorganic Med. Chem. Lett.* **1994**, *4* (16), 1913–1916.

(30) Kushida, N.; Watanabe, N.; Okuda, T.; Yokoyama, F.; Gyobu, Y.; Yaguchi, T. PF1270A, B and C, novel histamine H3 receptor ligands produced by Penicillium waksmanii PF1270. *J. Antibiot. (Tokyo).* **2007**, *60* (11), 667–673.

(31) Shi, Y.; Sheng, R.; Zhong, T.; Xu, Y.; Chen, X.; Yang, D.; Sun, Y.; Yang, F.; Hu, Y.; Zhou, N. Identification and characterization of ZEL-H16 as a novel agonist of the histamine H_3 receptor. *PLoS One* **2012**, *7* (8), e42185.

(32) Ghoshal, A.; Kumar, A.; Yugandhar, D.; Sona, C.; Kuriakose, S.; Nagesh, K.; Rashid, M.; Singh, S. K.; Wahajuddin, M.; Yadav, P. N.; Srivastava, A. K. Identification of novel β-lactams and pyrrolidinone derivatives as selective histamine-3 receptor (H3R) modulators as possible anti-obesity agents. *Eur. J. Med. Chem.* **2018**, *152*, 148–159.

(33) Igel, P.; Dove, S.; Buschauer, A. Histamine H_4 receptor agonists. *Bioorganic Med.*

Chem. Lett. **2010**, *20* (24), 7191–7199.

(34) Geyer, R.; Kaske, M.; Baumeister, P.; Buschauer, A. Synthesis and functional characterization of imbutamine analogs as histamine H_3 and H_4 receptor ligands. *Arch. Pharm. (Weinheim).* **2014**, *347* (2), 77–88.

(35) Kiss, R.; Keseru, G. M. Novel histamine H_4 receptor ligands and their potential therapeutic applications: an update. *Expert Opin. Ther. Pat.* **2014**, *24* (11), 1–13.

(36) Black, L. A.; Gfesser, G. A.; Cowart, M. D. 4-Substituted-2-amino-pyrimidine derivatives. US20100331294, 2010.

(37) Carceller González, E.; Medina Fuentes, E. M.; Martí Via, J.; Virgili Barnardó, M. 2-Amino-pyrimidine derivatives as histamine H_4 antagonists. WO2009068512, 2009.

(38) Cai, H.; Chavez, F.; Edwards, J. P.; Fitzgerald, A. E.; Liu, J.; Mani, N. S.; Neff, D. K.; Rizzolio, M. C.; Savall, B. M.; Smith, D. M.; Venable, J. D.; Jianmei, W.; Wolin, R. 2-Aminopyrimidine modulators of the histamine H_4 receptor. WO2008100565, 2010.

(39)   Sassano, M. F.; Doak, A. K.; Roth, B. L.; Shoichet, B. K. Colloidal aggregation causes inhibition of G protein-coupled receptors. *J. Med. Chem.* **2013**, *56* (6), 2406–2414.

(40)   Sirci, F.; Istyastono, E. P.; Vischer, H. F.; Kooistra, A. J.; Nijmeijer, S.; Kuijer, M.; Wijtmans, M.; Mannhold, R.; Leurs, R.; de Esch, I. J. P.; de Graaf, C. Virtual fragment screening: Discovery of histamine H_3 receptor ligands using ligand-based and protein-based molecular fingerprints. *J. Chem. Inf. Model.* **2012**, *52* (12), 3308–3324.

(41)   Kooistra, A. J.; Kuhne, S.; de Esch, I. J. P.; Leurs, R.; de Graaf, C. A structural chemogenomics analysis of aminergic GPCRs: Lessons for histamine receptor ligand design. *Br. J. Pharmacol.* **2013**, *170* (1), 101–126.

(42)   Jongejan, A.; Lim, H. D.; Smits, R. A.; de Esch, I. J. P.; Haaksma, E.; Leurs, R. Delineation of agonist binding to the human histamine H_4 receptor using mutational analysis, homology modeling, and ab initio calculations. *J. Chem. Inf. Model.* **2008**, *48* (7), 1455–1463.

(43) Shin, N.; Coates, E.; Murgolo, N. J.; Morse, K. L.; Bayne, M.; Strader, C. D.;

Monsma, F. J. Molecular modeling and site-specific mutagenesis of the histamine-

binding site of the histamine H$_4$ receptor. *Mol. Pharmacol.* **2002**, *62* (1), 38–47.

(44) Istyastono, E. P.; Nijmeijer, S.; Lim, H. D.; Stolpe, A. van de; Roumen, L.; Kooistra,

A. J.; Vischer, H. F.; de Esch, I. J. P.; Leurs, R.; de Graaf, C. Molecular

determinants of ligand binding modes in the histamine H$_4$ receptor: linking ligand-

based three-dimensional quantitative structure−activity relationship (3D-QSAR)

models to in silico guided receptor mutagenesis studies. *J. Med. Chem.* **2011**, *54*,

8136–8147.

(45) Uveges, A. J.; Kowal, D.; Zhang, Y.; Spangler, T. B.; Dunlop, J.; Semus, S.; Philip,

G. J. The role of transmembrane helix 5 in agonist binding to the human H3

receptor. *J. Pharmacol. Exp. Ther.* **2002**, *301* (2), 451–458.

(46) Shimamura, T.; Shiroishi, M.; Weyand, S.; Tsujimoto, H.; Winter, G.; Katritch, V.;

Abagyan, R.; Cherezov, V.; Liu, W.; Han, G. W.; Kobayashi, T.; Stevens, R. C.;

Iwata, S. Structure of the human histamine H1 receptor complex with doxepin.

Nature **2011**, *475* (7354), 65–72.

(47) Morse, K. L.; Behan, J.; Laz, T. M.; West, R. E. J.; Greenfeder, S. A.; Anthes, J. C.; Umland, S.; Wan, Y.; Hipkin, R. W.; Gonsiorek, W.; Shin, N.; Gustafson, E. L.; Qiao, X.; Wang, S.; Hedrick, J. A.; Greene, J.; Bayne, M.; Monsma, F. J. J. Cloning and characterization of a novel human histamine receptor. *J. Pharmacol. Exp. Ther.* **2001**, *269* (3), 1058–1066.

(48) Obach, R. S. Prediction of human clearance of twenty-nine drugs from hepatic microsomal intrinsic clearance data: An examination of in vitro half-life approach and nonspecific binding to microsomes. *Drug Metab. Dispos.* **1999**, *27* (11), 1350–1359.

(49) Lin, J. H.; Lu, A. Y. H. Inhibition and induction of cytochrome P450 and the clinical implications. *Clin. Pharmacokinet.* **1998**, *35* (5), 361–390.

(50) Provensi, G.; Costa, A.; Izquierdo, I.; Blandina, P.; Passani, M. B. Brain histamine modulates recognition memory: possible implications in major cognitive disorders. *Br. J. Pharmacol.* [Online early access]. DOI: 10.1111/bph.14478. Published

Online: Augustus 21, 2018.

(51) Prast, H.; Argyriou, A.; Philippu, A. Histaminergic neurons facilitate social memory

in rats. *Brain Res.* **1996**, *734* (1–2), 316–318.

(52) Provensi, G.; Passani, M. B.; Costa, A.; Izquierdo, I.; Blandina, P. Neuronal

histamine and the memory of emotionally salient events. *Br. J. Pharmacol.* [Online

early access]. DOI: 10.1111/bph.14476. Published Online: Augustus 15, 2018.

(53) Parmentier, R.; Anaclet, C.; Guhennec, C.; Brousseau, E.; Bricout, D.; Giboulot, T.;

Bozyczko-Coyne, D.; Spiegel, K.; Ohtsu, H.; Williams, M.; Lin, J. S. The brain H$_3$-

receptor as a novel therapeutic target for vigilance and sleep-wake disorders.

Biochem. Pharmacol. **2007**, *73* (8), 1157–1171.

(54) Yokoyama, F.; Yamauchi, M.; Oyama, M.; Okuma, K.; Onozawa, K.; Nagayama,

T.; Shinei, R.; Ishikawa, M.; Sato, Y.; Kakui, N. Anxiolytic-like profiles of histamine

H3 receptor agonists in animal models of anxiety: a comparative study with

antidepressants and benzodiazepine anxiolytic. *Psychopharmacology (Berl).* **2009**,

205 (2), 177–187.

(55)   Schneider, E. H.; Neumann, D.; Seifert, R. Histamine H$_4$-receptor expression in the

brain? *Naunyn. Schmiedebergs. Arch. Pharmacol.* **2015**, *388* (1), 5–9.

(56)   Sanna, M. D.; Ghelardini, C.; Thurmond, R. L.; Masini, E.; Galeotti, N. Behavioural

phenotype of histamine H$_4$ receptor knockout mice: Focus on central neuronal

functions. *Neuropharmacology* **2017**, *114*, 48–57.

(57)   Blandina, P.; Giorgetti, M.; Bartolini, L.; Cecchi, M.; Timmerman, H.; Leurs, R.;

Pepeu, G.; Giovannini, M. G. Inhibition of cortical acetylcholine release and

cognitive performance by histamine H$_3$ receptor activation in rats. *Br. J. Pharmacol.*

1996, *119* (8), 1656–1664.

(58)   Nijmeijer, S.; Engelhardt, H.; Schultes, S.; van de Stolpe, A. C.; Lusink, V.; de

Graaf, C.; Wijtmans, M.; Haaksma, E. E. J.; de Esch, I. J. P.; Stachurski, K.;

Vischer, H. F.; Leurs, R. Design and pharmacological characterization of

VUF14480, a covalent partial agonist that interacts with cysteine 98$^{3.36}$ of the

human histamine H$_4$ receptor. *Br. J. Pharmacol.* **2013**, *170* (1), 89–100.

(59)   Mocking, T. A. M.; Verweij, E. W. E.; Vischer, H. F.; Leurs, R. Homogeneous, real-

time NanoBRET binding assays for the histamine H_3 and H_4 receptors on living

cells. *Mol. Pharmacol.* **2018**, *94* (6), 1371–1381.

(60) Hauwert, N. J.; Mocking, T. A. M.; Da Costa Pereira, D.; Lion, K.; Huppelschoten,

Y.; Vischer, H. F.; de Esch, I. J. P.; Wijtmans, M.; Leurs, R. A photoswitchable

agonist for the histamine H_3 receptor, a prototypic family a G-protein-coupled

receptor. *Angew. Chemie - Int. Ed.* **2019**, *58* (14), 4531–4535.

(61) Cheng, Y.; Prusoff, W. H. Relation between the inhibiton constant (Ki) and the

concentration of inhibitor which causes 50 percent inhibiton (IC50) of an enzymatic

reaction. *Biochem. Pharmacol.* **1973**, *22* (23), 3099–3108.

(62) Huang, Z.; Li, H.; Zhang, Q.; Tan, X.; Lu, F.; Liu, H.; Li, S. Characterization of

preclinical in vitro and in vivo pharmacokinetics properties for KBP-7018, a new

tyrosine kinase inhibitor candidate for treatment of idiopathic pulmonary fibrosis.

Drug Des. Devel. Ther. **2015**, *9*, 4319–4328.

(63) Smith, R.; Jones, R. D. O.; Ballard, P. G.; Griffiths, H. H. Determination of

microsome and hepatocyte scaling factors for in vitro/in vivo extrapolation in the rat

and dog. *Xenobiotica* **2008**, *38* (11), 1386–1398.

(64) Isberg, V.; de Graaf, C.; Bortolato, A.; Cherezov, V.; Katritch, V.; Marshall, F. H.;

Mordalski, S.; Pin, J.-P.; Stevens, R. C.; Vriend, G.; Gloriam, D. E. Generic GPCR

residue numbers - aligning topology maps minding the gaps. *Trends Pharmacol*

Sci. **2016**, *36* (1), 22–31.

(65) Sali, A. Comparative protein modeling by satisfaction of spatial restraints. *Mol. Med.*

Today **1995**, *1* (6), 270–277.

(66) Bateman, A.; Martin, M. J.; O'Donovan, C.; Magrane, M.; Alpi, E.; Antunes, R.; Bely,

B.; Bingley, M.; Bonilla, C.; Britto, R.; Bursteinas, B.; Bye-AJee, H.; Cowley, A.; Da

Silva, A.; De Giorgi, M.; Dogan, T.; Fazzini, F.; Castro, L. G.; Figueira, L.; Garmiri,

P.; Georghiou, G.; Gonzalez, D.; Hatton-Ellis, E.; Li, W.; Liu, W.; Lopez, R.; Luo, J.;

Lussi, Y.; MacDougall, A.; Nightingale, A.; Palka, B.; Pichler, K.; Poggioli, D.;

Pundir, S.; Pureza, L.; Qi, G.; Rosanoff, S.; Saidi, R.; Sawford, T.; Shypitsyna, A.;

Speretta, E.; Turner, E.; Tyagi, N.; Volynkin, V.; Wardell, T.; Warner, K.; Watkins,

X.; Zaru, R.; Zellner, H.; Xenarios, I.; Bougueleret, L.; Bridge, A.; Poux, S.;

Redaschi, N.; Aimo, L.; ArgoudPuy, G.; Auchincloss, A.; Axelsen, K.; Bansal, P.;

Baratin, D.; Blatter, M. C.; Boeckmann, B.; Bolleman, J.; Boutet, E.; Breuza, L.;

Casal-Casas, C.; De Castro, E.; Coudert, E.; Cuche, B.; Doche, M.; Dornevil, D.;

Duvaud, S.; Estreicher, A.; Famiglietti, L.; Feuermann, M.; Gasteiger, E.; Gehant,

S.; Gerritsen, V.; Gos, A.; Gruaz-Gumowski, N.; Hinz, U.; Hulo, C.; Jungo, F.; Keller,

G.; Lara, V.; Lemercier, P.; Lieberherr, D.; Lombardot, T.; Martin, X.; Masson, P.;

Morgat, A.; Neto, T.; Nouspikel, N.; Paesano, S.; Pedruzzi, I.; Pilbout, S.; Pozzato,

M.; Pruess, M.; Rivoire, C.; Roechert, B.; Schneider, M.; Sigrist, C.; Sonesson, K.;

Staehli, S.; Stutz, A.; Sundaram, S.; Tognolli, M.; Verbregue, L.; Veuthey, A. L.;

Wu, C. H.; Arighi, C. N.; Arminski, L.; Chen, C.; Chen, Y.; Garavelli, J. S.; Huang,

H.; Laiho, K.; McGarvey, P.; Natale, D. A.; Ross, K.; Vinayaka, C. R.; Wang, Q.;

Wang, Y.; Yeh, L. S.; Zhang, J. UniProt: The universal protein knowledgebase.

Nucleic Acids Res. **2017**, *45* (D1), D158–D169.

(67)   Sadowski, J.; Gasteiger, J.; Klebe, G. Comparison of automatic three-dimensional

model builders using 639 X-ray structures. *J. Chem. Inf. Comput. Sci.* **1994**, *34* (4),

1000–1008.

(68)   ChemAxon, L. Calculator, version 5.1.4. In Budapest, Hungary, 1998-2018.

(69)   Korb, O.; Stützle, T.; Exner, T. E. An ant colony optimization approach to flexible

protein–ligand docking. *Swarm Intell.* **2007**, *1* (2), 115–134.

(70)   Marcou, G.; Rognan, D. Optimizing fragment and scaffold docking by use of

molecular interaction fingerprints. *J. Chem. Inf. Model.* **2007**, *47* (1), 195–207.

(71)   de Graaf, C.; Kooistra, A. J.; Vischer, H. F.; Katritch, V.; Kuijer, M.; Shiroishi, M.;

Iwata, S.; Shimamura, T.; Stevens, R. C.; de Esch, I. J. P.; Leurs, R. Crystal

structure-based virtual screening for fragment-like ligands of the human histamine

H_1 receptor. *J. Med. Chem.* **2011**, *54* (23), 8195–8206.

(72)   Jakalian, A.; Jack, D. B.; Bayly, C. I. Fast, efficient generation of high-quality atomic

charges. AM1-BCC model: II. Parameterization and validation. *J. Comput. Chem.*

2002, *23* (16), 1623–1641.

(73)   Berendsen, H. J. C.; van der Spoel, D.; van Drunen, R. GROMACS: A message-

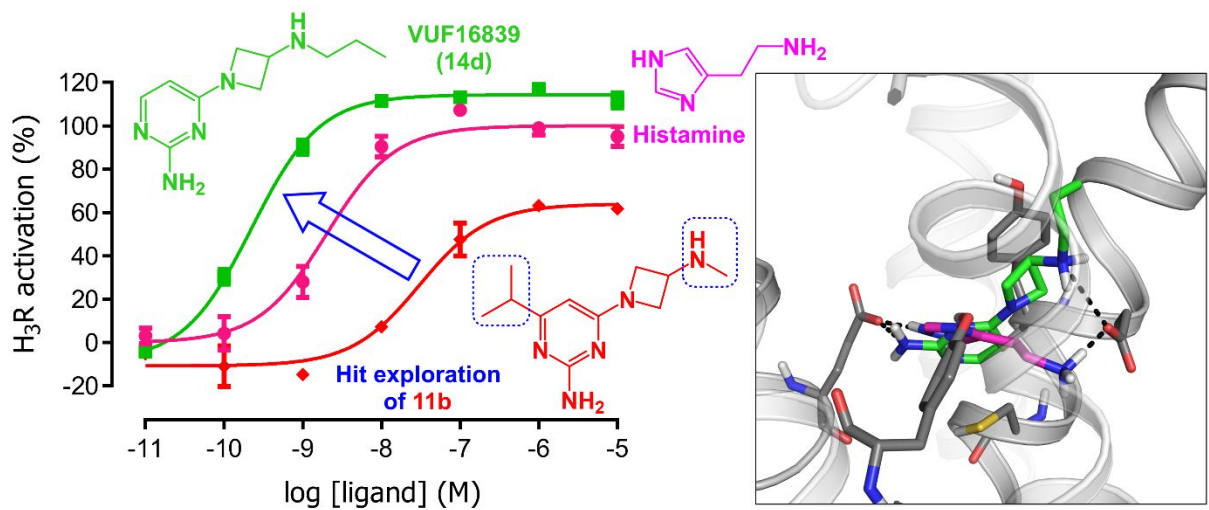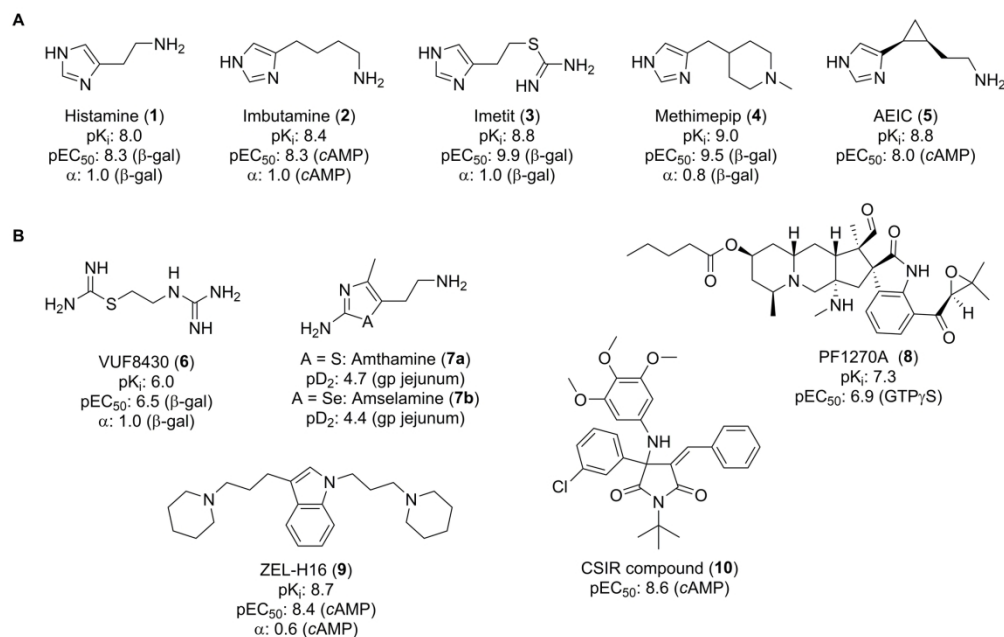passing parallel molecular dynamics implementation. *Comput. Phys. Commun.* **1995**, *91* (1–3), 43–56.

(74) Cordomí, A.; Caltabiano, G.; Pardo, L. Membrane protein simulations using AMBER force field and Berger lipid parameters. *J. Chem. Theory Comput.* **2012**, *8* (3), 948–958.

(75) Roessler, W. G.; Brewer, C. R. Permanent turbidity standards. *Appl. Microbiol.* **1967**, *15* (5), 1114–1121.

(76) Baell, J. B.; Holloway, G. A. New substructure filters for removal of pan assay interference compounds (PAINS) from screening libraries and for their exclusion in bioassays. *J. Med. Chem.* **2010**, *53* (7), 2719–2740.

TABLE OF CONTENTS GRAPHIC

1
2
3
4
5
6
7
8
9
10
11
12
13
14
15
16
17
18
19
20
21
22
23
24
25
26
27
28
29
30
31
32
33
34
35
36
37
38
39
40
41
42
43
44
45
46
47
48
49
50
51
52
53
54
55
56
57
58
59
60

A

Histamine (**1**)
pK$_i$: 8.0
pEC$_{50}$: 8.3 (β-gal)
α: 1.0 (β-gal)

Imbutamine (**2**)
pK$_i$: 8.4
pEC$_{50}$: 8.3 (cAMP)
α: 1.0 (cAMP)

Imetit (**3**)
pK$_i$: 8.8
pEC$_{50}$: 9.9 (β-gal)
α: 1.0 (β-gal)

Methimepip (**4**)
pK$_i$: 9.0
pEC$_{50}$: 9.5 (β-gal)
α: 0.8 (β-gal)

AEIC (**5**)
pK$_i$: 8.8
pEC$_{50}$: 8.0 (cAMP)

B

VUF8430 (**6**)
pK$_i$: 6.0
pEC$_{50}$: 6.5 (β-gal)
α: 1.0 (β-gal)

A = S: Amthamine (**7a**)
pD$_2$: 4.7 (gp jejunum)
A = Se: Amselamine (**7b**)
pD$_2$: 4.4 (gp jejunum)

PF1270A (**8**)
pK$_i$: 7.3
pEC$_{50}$: 6.9 (GTPγS)

CSIR compound (**10**)
pEC$_{50}$: 8.6 (cAMP)

ZEL-H16 (**9**)
pK$_i$: 8.7
pEC$_{50}$: 8.4 (cAMP)
α: 0.6 (cAMP)

A) Representative imidazole H$_3$R agonists. Activities are extracted from Igel *et al*.[33], Govoni *et al*.[18] and Kazuta *et al*.[12] **B**) Published non-imidazole H$_3$R (partial) agonists.[27–32] Unless mentioned otherwise, compounds were tested on the human receptor. α: intrinsic activity compared to histamine. β-gal: CRE-β-galactosidase reporter gene assay; cAMP: forskolin-stimulated cAMP accumulation assay.

210x133mm (300 x 300 DPI)
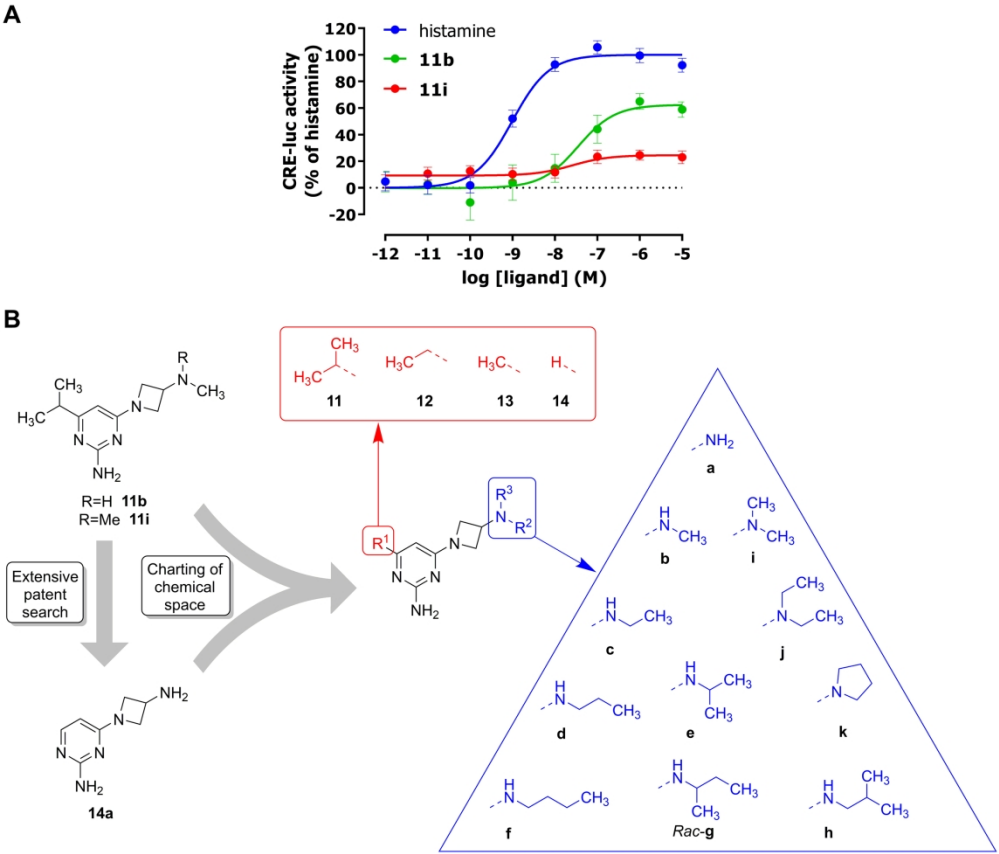
A) Initial functional data of compound **11b** and **11i** compared to histamine, as obtained by ligand-induced activation of hH$_3$R expressed on HEK293T cells measured by CRE-luc reporter gene assay. Shown is a representative graph of at least 3 experiments performed in triplicate. Data are mean ± S.D. **B**) Structures of **11b** and **11i**, the closest relevant structure (**14a**) resulting from a subsequent extensive patent search and the compound set designed for the current study.

228x196mm (300 x 300 DPI)
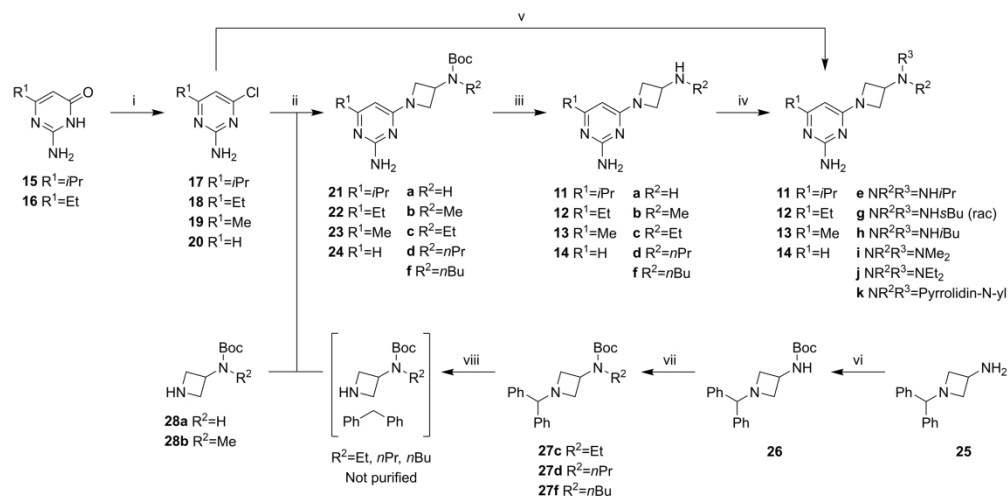
Reagents and conditions: i) POCl$_3$, 110 °C, 3h, 26-52 %; ii) DIPEA, dioxane or NMP, □W, 120 - 150 °C, 0.5 - 2 h, 27-50 % (**a** and **b**) or 35-71 % (**c, d** and **f**, two steps from benzhydryl deprotection); iii) HCl, DCM, MeOH, rt - 50 °C, 3 h - overnight, 10 % - quant.; iv) aldehyde/ketone, AcOH, NaHB(OAc)$_3$, DCM, MeOH, rt, 3 h - overnight, 16-44 %; or 1,4-diiodobutane, K$_2$CO$_3$, MeCN, reflux, 16 h, 9 %; v) N,N-dimethylazetidin-3-amine dihydrochloride, DIPEA, dioxane, μW, 150 °C, 30 min, 65 %; vi) di-tert-butyl dicarbonate, TEA, THF, rt, overnight, 63 %; vii) NaH, R^{2}I, THF, 0 °C - rt, overnight, 28-58 %; viii) H$_2$, Pd/C, MeOH, EtOH, rt - 60 °C, 1 h - overnight, not purified and used crude.
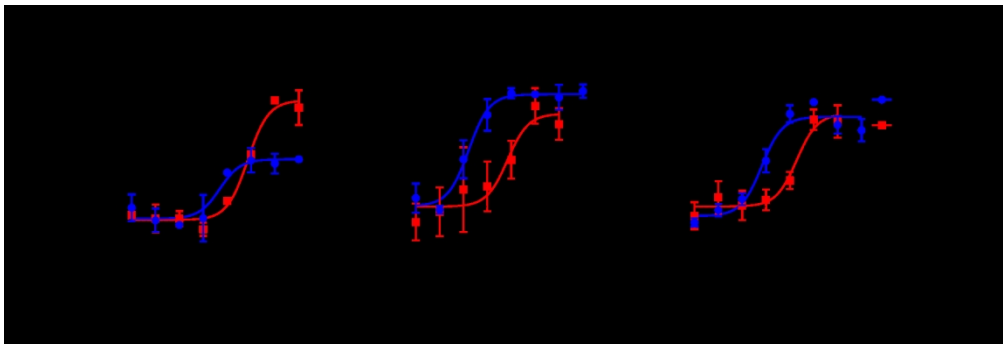
250x124mm (300 x 300 DPI)
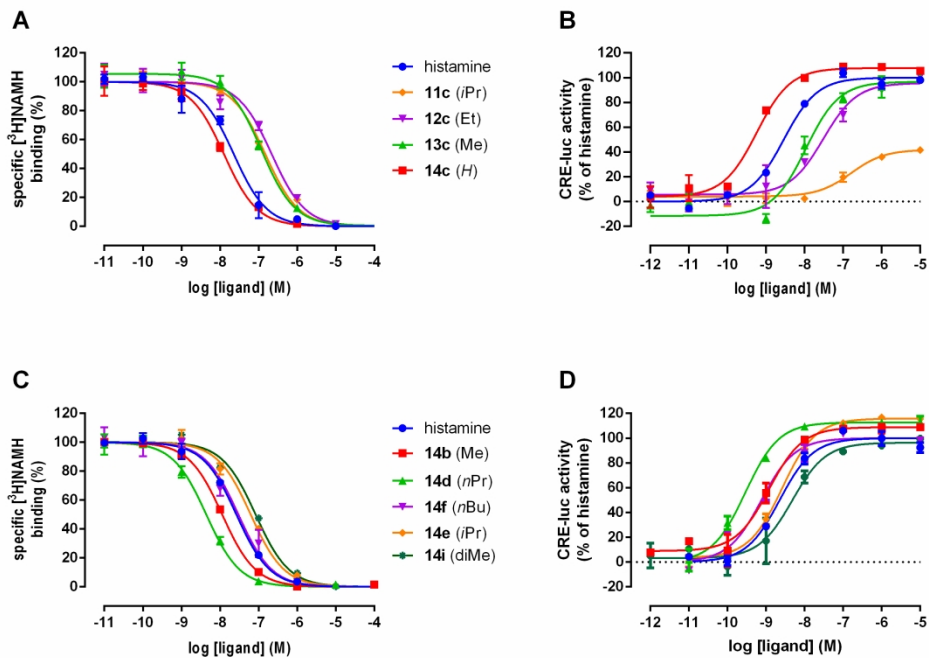
Representative Structure-Affinity (**A**, **C**) and Structure-Function relationship (**B**, **D**) effects selected from Table 1. (**A**, **B**) Different R^1 substituents with R^2 = Et and R^3 = H (**11c**, **12c**, **13c**, **14c**); (C, D) Different R^2 and R^3 substituents with R^1 = H (**14b**, **14d**, **14e**, **14f**, **14i**). Shown is a representative graph of at least 3 experiments performed in triplicate. Data are mean ± S.D.
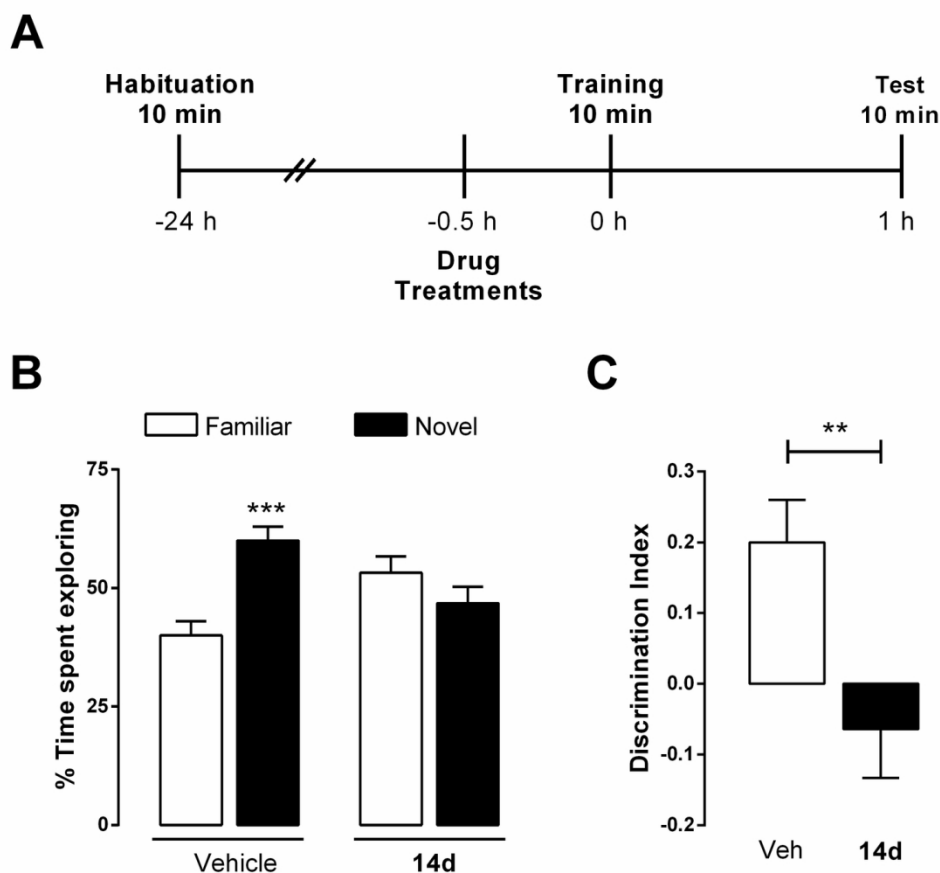
263x182mm (300 x 300 DPI)
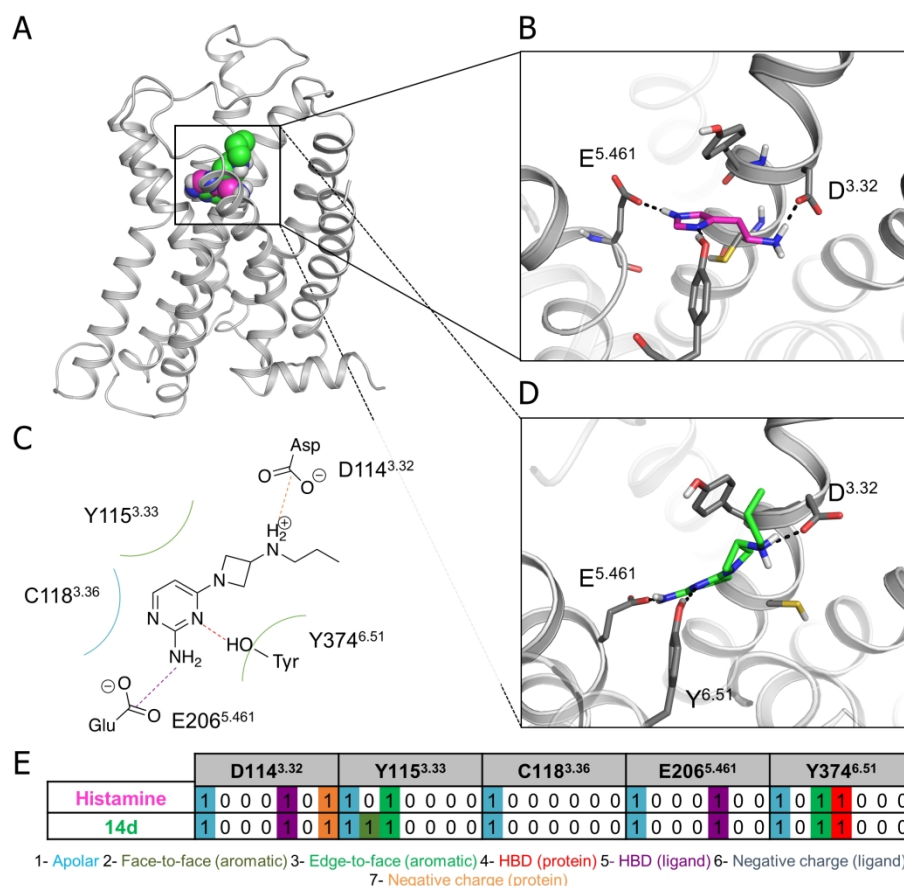
Predicted binding mode of **14d**. **A**) Overview of the H3R homology model based on the H1R crystal structure (PDB ID: 3RZE).[46] The experimentally validated binding mode of histamine (magenta) is shown in more detail in (**B**) and the predicted binding mode of **14d** (green) is schematically represented in (**C**) and shown in more detail in (**D**). Interaction fingerprint representations of histamine and compound **14d** are shown in (**E**), where a one represents the presence of an interaction according to the color coding: blue for apolar, dark green for face-to-face aromatic, green for edge-to-face aromatic, red for protein hydrogen bond donor, purple for ligand hydrogen bond donor, grey for ligand negative charge, and orange for protein negative charge.

199x184mm (300 x 300 DPI)

1
2
3
4
5
6
7
8
9
10
11
12
13
14
15
16
17
18
19
20
21
22
23
24
25
26
27
28
29
30
31
32
33
34
35
36
37
38
39
40
41
42
43
44
45
46
47
48
49
50
51
52
53
54
55
56
57
58
59
60

(**A**) Dose-dependent Gαi activation by **14d** and histamine as measured by [^{35}S]GTPγS accumulation on HEK293T cell homogenates expressing the hH$_3$R. (**B**, **C**) Dose-response curves of **14d** and histamine for ligand-induced activation of mH$_3$R (**B**) and mH$_4$R (**C**) expressed on HEK293T cells as measured by CRE-luciferase reporter gene assay. Representative graphs of at least three experiments performed in triplicate are shown. Data are mean ± S.D.

163x55mm (300 x 300 DPI)

A

Habituation
10 min

Training
10 min

Test
10 min

-24 h   -0.5 h   0 h   1 h

**Drug
Treatments**

B

□ Familiar   ■ Novel

% Time spent exploring

***

75

50

25

0

Vehicle   **14d**

C

**

Discrimination Index

0.3

0.2

0.1

0.0

-0.1

-0.2

Veh   **14d**

Compound **14d** impairs social recognition in mice. **A**) Schematic drawings showing the sequence of procedures and treatment administrations. **B**) Results are calculated as means of individual percentage of time spent exploring familiar (white columns) and novel (black columns) social stimuli. ***P<0.001 vs. respective familiar subject (Two-way ANOVA and Bonferroni's MCT). **C**) Discrimination index calculated according to the formula tN-tF/tN+tF. **P<0.01 vs. vehicle (unpaired t-test). Shown are means ± S.E.M. of 10-11 animals per experimental group.

135x127mm (300 x 300 DPI)